Check for updates

J. Appl. Probab. **62,** 972–996 (2025)
*doi:*10.1017/jpr.2024.105

INTERACTING URNS ON DIRECTED NETWORKS WITH NODE-DEPENDENT SAMPLING AND REINFORCEMENT

GURSHARN KAUR,* *University of Virginia*
NEERAJA SAHASRABUDHE,** *Indian Institute of Science Education and Research*

Abstract

We consider interacting urns on a finite directed network, where both sampling and reinforcement processes depend on the nodes of the network. This extends previous research by incorporating node-dependent sampling and reinforcement. We classify the sampling and reinforcement schemes, as well as the networks on which the proportion of balls of either colour in each urn converges almost surely to a deterministic limit. We also investigate conditions for achieving synchronisation of the colour proportions across the urns and analyse fluctuations under specific conditions on the reinforcement scheme and network structure.

Keywords: Reinforcement; stochastic approximation; central limit theorem; synchronisation

2010 Mathematics Subject Classification: Primary 60K35
Secondary 60F05; 90B15

1. Introduction

Interacting urn models have been studied extensively in recent times [2, 3, 6, 7, 11, 12, 13]. In an interacting urn model, each urn is reinforced based on the sampling of balls from itself or other urns in the system. Such models exhibit interesting asymptotic behaviour and have applications across various fields, such as opinion dynamics [9] and in analysing contagion over a network [14]. In addition to convergence, the phenomenon of synchronisation (or consensus) is also of interest, especially for exploring applications of these models in opinion dynamics. Synchronisation refers to the convergence of the proportion of balls of each colour to the same limit across all urns. A special class of interacting models was studied in [13], where the authors examined a two-colour multi-urn process where the evolution of each urn depends on itself (with probability p) as well as on all the other urns in the system (with probability $1-p$). The interaction aspect of such models was extended to study urn processes (or, more generally, stochastic processes taking values in [0,1]) on finite networks in [1]. The model studied in [12] extends the interactions described in [13] by incorporating a non-linear sampling probability that depends on a function of the number of balls of each colour. The author obtains conditions on the function so that with probability 1 eventually only balls of one colour are added to the

Received 6 January 2024; accepted 2 November 2024.
* Postal address: Biocomplexity Institute, University of Virginia, Charlottesville, USA. 22904. Email: gursharn@virginia.edu
** Postal address: Department of Mathematical Sciences, IISER Mohali, Knowledge city, Sector 81, SAS Nagar, Manauli PO 140306, India. Email: neeraja@iisermohali.com

© The Author(s), 2025. Published by Cambridge University Press on behalf of Applied Probability Trust. This is an Open Access article, distributed under the terms of the Creative Commons Attribution licence (https://creativecommons.org/licenses/by/4.0/), which permits unrestricted re-use, distribution, and reproduction in any medium, provided the original work is properly cited.

https://doi.org/10.1017/jpr.2024.105 Published online by Cambridge University Press

urns. In [7] the authors consider interacting urns where the reinforcement dynamics depend on the average composition in the system as well as a non-linear function of the individual urn composition and show that in some cases there can be no synchronisation even when there is an interaction between nodes. Further, the authors in [11] propose a system of reinforced stochastic processes, interacting through an additional collective reinforcement of mean-field type.

In this paper, we extend the work of [1, 10] by considering urns with balls of two colours on a finite directed network $\mathcal{G} = (V, \mathcal{E})$, such that each urn i uses a node-dependent reinforcement matrix R_i. That is, at each time step, a ball is drawn from each urn i, and the urn reinforces its out-neighbours based on the colour of the drawn ball. If a white ball is drawn, it adds $[R_i]_{1,1}$ white balls and $[R_i]_{1,2}$ black balls to each of its out-neighbours; if a black ball is drawn, it adds $[R_i]_{2,1}$ white balls $[R_i]_{2,2}$ black balls to its out-neighbours. We assume that each reinforcement matrix is balanced, i.e. the row sums of R_i are constant (say m_i).

We classify the urns or nodes as either *Pólya* or *non-Pólya* type based on the nature of their reinforcement matrices. By considering *node-dependent* reinforcement, this paper extends the work of [10], where the asymptotic properties of a similar interacting urn model with a fixed reinforcement scheme are studied.

In addition to node-based reinforcement, we also consider node-based sampling, wherein at each time step the probability of drawing a white ball from urn i is the fraction of white balls in the urn at that time with probability q_i, and the fraction of black balls with probability $1 - q_i$. In other words, each urn has a tendency (quantified by q_i) to 'lie' about its actual configuration. When q_i is either 0 or 1, it results in either preferential (where a white ball is drawn with probability proportional to its fraction) or de-preferential sampling (where a white ball is drawn with probability proportional to the fraction of black balls) respectively. This type of linear de-preferential sampling, where a more frequent colour is less likely to be sampled, has been studied before in [4, 9] for a single urn with multiple colours, where the authors showed that, depending on the reinforcement matrix, the colour proportions in the urn converge almost surely to a deterministic vector, and derived central limit theorem type results.

In this paper we classify the reinforcement types and graph structures that ensure the proportion of balls of each colour across all urns converges almost surely to a deterministic limit, thus generalising the results in [10]. Our results show that a deterministic limit exists if there is at least one node with $0 < q_i < 1$, or the graph and the reinforcement matrices are such that the influence of the stubborn urn (a node with zero in-degree) or a non-Pólya type urn permeates the entire graph. Specifically, on a strongly connected graph, the presence of a single node with non-Pólya type reinforcement is sufficient to guarantee a deterministic limit for the proportion of balls of either colour across all urns. When all nodes are of Pólya type, we show that the presence of de-preferential nodes can still yield a deterministic limit. Further, when $q_i \in \{0, 1\}$ for all i, we classify graphs based on the relative positioning of preferential and de-preferential nodes, where a deterministic limit is feasible. We also derive general conditions for synchronisation, where the proportion of balls of either colour converges to the same deterministic limit in each urn. Finally, we state and prove central limit theorem (CLT) type results for the fluctuation of the proportion of a colour in each urn around its limit.

In the next section we provide an overview of the interacting urn process. For a matrix $Q \in \mathbb{R}^{d\times d}$ and subsets $S, F \subseteq [d] := \{1, 2, \ldots, d\}$, we use the notation Q_{SF} to represent the $|S| \times |F|$ submatrix obtained by selecting elements from the index set $S \times F$. For simplicity, we write Q_S instead of Q_{SS}. Throughout the paper, $\mathbf{1}$ denotes a row vector of appropriate dimension with all elements equal to 1.

https://doi.org/10.1017/jpr.2024.105 Published online by Cambridge University Press

2. Interacting urn process

Let $\mathcal{G} = (V, \mathcal{E})$ be a directed network, where $V = [N]$ denotes the set of nodes and $\mathcal{E}$ represents the set of directed edges. For nodes i and j in V, we use $i \to j$ to indicate a directed edge from i to j, and $i \rightsquigarrow j$ denotes a path $i = i_0 \to i_1 \to \cdots \to i_{k-1} \to i_k = j$ from i to j, where $i_1, \ldots, i_{k-1} \in V$. For a subset $U \subseteq V$, $v \to U$ means there exists at least one node $u \in U$ such that $v \to u$. The in-degree and out-degree of a node i are denoted by $d_i^{\text{in}} := |\{j \in V : j \to i\}|$ and $d_i^{\text{out}} := |\{j \in V : i \to j\}|$ respectively. The in-neighbourhood of node i is $N_i := \{j \in V : j \to i\}$. Throughout this paper, we assume that $\mathcal{G}$ is weakly connected.

Following the approach in [10], the node set V is partitioned into two disjoint sets: the set of stubborn nodes denoted by S and the set of flexible nodes denoted by F. Specifically, we have $V = S \cup F$, where $S = \{i \in V : d_i^{\text{in}} = 0\}$ represents the stubborn nodes and $F = \{i \in V : d_i^{\text{in}} > 0\}$ represents the flexible nodes. Without loss of generality, we assume that the nodes labelled $1, \ldots, |F|$ belong to the flexible set F. By adopting this labelling convention, the adjacency matrix A, where $[A]_{i,j} = \mathbb{I}_{\{i \to j\}}$, has the following block structure:

$$\begin{pmatrix} A_F & \mathbf{0} \\ A_{SF} & \mathbf{0} \end{pmatrix}.$$

Suppose each node $i \in V$ has an urn that contains balls of two colours, white and black. Let (W_i^t, B_i^t) be the configuration of the urn at node i, where W_i^t and B_i^t denote the number of white and black balls. Let $T_i^t = W_i^t + B_i^t$ be the total number of balls in urn i at time t. Define $\mathbf{Z}^t = (Z_1^t, \ldots, Z_N^t)$, where $Z_i^t = W_i^t/(W_i^t + B_i^t)$, as the fraction of white balls in urn i at time $t \geq 0$. Given the configuration $(W_i^t, B_i^t)_{i \in V}$ at time t, the configuration of each urn is updated at time $t + 1$ using the following two steps:

(i). **Sampling:** A ball is selected from each urn with a probability that is a convex combination of the proportion of white balls and the proportion of black balls. Let χ_i^t be the indicator variable for the event that a white ball is drawn from the urn at node i at time t. Then, conditioned on $\mathcal{F}_t = \sigma(\mathbf{Z}^0, \mathbf{Z}^1, \ldots, \mathbf{Z}^t)$, $\{\chi_i^{t+1}\}_{i \in V}$ are independent random variables such that

$$\chi_i^{t+1} = \begin{cases} 1 & \text{with probability } q_i Z_i^t + (1 - q_i)(1 - Z_i^t), \\ 0 & \text{with probability } (1 - q_i) Z_i^t + q_i^t (1 - Z_i^t), \end{cases} \tag{1}$$

where $q_i \in [0, 1]$ for each node i, i.e. given $\mathcal{F}_t$, χ_i^{t+1} is a $\text{Ber}((2q_i - 1)Z_i^t + (1 - q_i))$ random variable. We call this process *linear sampling* with parameter q_i. Note that, when $q_i = \frac{1}{2}$, the sampling is independent of the urn configuration. A node i is termed *preferential* if $q_i = 1$ and *de-preferential* if $q_i = 0$. Let $\mathcal{P}$, $\mathcal{D}$ denote the set of nodes with preferential and de-preferential sampling respectively.
Let $\chi^{t+1} = (\chi_1^{t+1}, \ldots, \chi_N^{t+1})$. Define $\mathcal{I} := \text{Diag}\,(2q_1 - 1, \ldots, 2q_N - 1)$ and $\Theta^t := \text{Diag}\,((Z_1^t - 1/2)^2, \ldots, (Z_N^t - 1/2)^2)$. Then, we have

$$\mathbb{E}[\chi^{t+1} \mid \mathcal{F}_t] = \mathbf{Z}^t \mathcal{I} + (\mathbf{1} - \mathbf{q}), \tag{2}$$

$$\text{Var}\,(\chi^{t+1} \mid \mathcal{F}_t) = -\Theta^t \mathcal{I}^2 + \frac{1}{4} I. \tag{3}$$

https://doi.org/10.1017/jpr.2024.105 Published online by Cambridge University Press

After observing the vector χ^{t+1}, the balls are returned to their respective urns along with a specified number of white and black balls, according to the reinforcement scheme described in the next step.

(ii). **Reinforcement:** Let $m_i \in \mathbb{Z}_{\geq 0}$ and $\alpha_i, \beta_i \in \{0, 1, \ldots, m_i\}$ be fixed non-negative integers for each node $i \in V$. If a white ball is selected from the urn at node i (in the sampling step), α_i white balls and $m_i - \alpha_i$ black balls are added to each urn j such that $i \to j$. On the other hand, if a black ball is selected from the urn at node i, $m_i - \beta_i$ white balls and β_i black balls are added to each urn at each node j such that $i \to j$. In other words, the urn at node i reinforces its out-neighbours according to the reinforcement matrix

$$R_i = \begin{pmatrix} \alpha_i & m_i - \alpha_i \\ m_i - \beta_i & \beta_i \end{pmatrix}.$$

We classify the type of reinforcement by node i as follows.

- Pólya type if $\alpha_i = \beta_i = m_i$, which corresponds to $R_i = m_i I$;
- non-Pólya type if $0 < \alpha_i + \beta_i < 2m_i$.

The interacting urn dynamics (defined by the sampling and reinforcement steps) can be expressed by the following recursive relations:

$$\begin{aligned} W_i^{t+1} &= W_i^t + \sum_{j \in N_i} \left[\alpha_j \chi_j^{t+1} + (m_j - \beta_j)\left(1 - \chi_j^{t+1}\right)\right], \\ B_i^{t+1} &= B_i^t + \sum_{j \in N_i} \left[m_j - \alpha_j \chi_j^{t+1} + \beta_j \left(1 - \chi_j^{t+1}\right)\right] \quad \text{for all } i \in V. \end{aligned} \tag{4}$$

Note that, although we consider $m_i, \alpha_i, \beta_i \in \mathbb{Z}_{\geq 0}$, the results in this paper extend to all balanced matrices with entries in $\mathbb{R}_{\geq 0}$. Furthermore, the urns at stubborn nodes are not reinforced, and therefore their configurations remain unchanged throughout the process.

Before we proceed to state and prove our main results, we fix some notation. Define $a_i = \alpha_i / m_i$ and $b_i = \beta_i / m_i$. Let $\mathbf{a} = (a_1, \ldots, a_N)$ and $\mathbf{b} = (b_1, \ldots, b_N)$. The total reinforcement at node i is $\overline{m}_i = \sum_{j \in N_i} m_j$. We also define the diagonal matrices $B = \text{Diag}\,(a_1 + b_1 - 1, \ldots, a_N + b_N - 1)$, $\mathbf{T}^t = \text{Diag}\,(T_1^t, \ldots, T_N^t)$, $M = \text{Diag}\,(m_1, \ldots, m_N)$, and $\overline{M} = \text{Diag}\,(\overline{m}_1, \ldots, \overline{m}_{|F|}, \mathbf{0}_S)$, where $\overline{m}_i = 0$ for every $i \in S$. Finally, the scaled adjacency matrix is defined as $\widetilde{A} = MA\overline{M}^{-1}$, where $\overline{M}^{-1} = \text{Diag}\,(\overline{m}_1^{-1}, \ldots, \overline{m}_{|F|}^{-1}, \mathbf{0}_S)$.

2.1. Equivalence in node-based and node-independent sampling

Throughout this paper, we have omitted the case where $\alpha_i + \beta_i = 0$ or $\alpha_i + \beta_i = 2m_i$, except for a specific case covered under Theorem 1. The case where $\alpha_i + \beta_i = 0$ is when both values are zero, which leads to the reinforcement matrix

$$\begin{pmatrix} 0 & m_i \\ m_i & 0 \end{pmatrix}.$$

It is worth noting that preferential sampling with this reinforcement matrix is equivalent to de-preferential sampling with Pólya type reinforcement. However, as discussed later, this reinforcement scheme may not always lead to a deterministic limit. In this paper our focus is

https://doi.org/10.1017/jpr.2024.105 Published online by Cambridge University Press

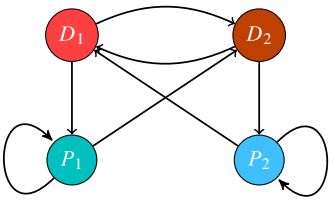


FIGURE 1. The exploration process for the graph partition $\mathcal{G}(P_1, P_2, D_1, D_2)$, as described in Steps 8 to 11 of Algorithm 1 (Appendix A). The arrows represent the directed edges where, for instance, an arrow from D_1 to P_1 means that there exist $u \in D_1$ and $v \in P_1$ such that $u \to v$ in $\mathcal{G}$.

to analyse the cases where $\mathbf{Z}^t$ converges to a deterministic limit, so we do not address these specific cases.

More generally, for any node, linear sampling with parameter q_i and reinforcement with R_i is equivalent to uniform sampling with reinforcement using the matrix

$$\begin{pmatrix} \alpha_i q_i + (m_i - \beta_i)(1 - q_i) & (m_i - \alpha_i)q_i + \beta_i(1 - q_i) \\ \alpha_i(1 - q_i) + (m_i - \beta_i)q_i & (m_i - \alpha_i)(1 - q_i) + \beta_i q_i \end{pmatrix}.$$

Such node-dependent reinforcement models, where each node uses its own reinforcement scheme, have not been studied before. Despite equivalence through this coupling, we study the processes by separating node-based sampling and node-based reinforcement for clarity and application purposes. This distinction is important for extending existing models of de-preferential sampling (see [4]) to interacting urns and for future exploration of non-linear sampling schemes. The non-linear sampling has been studied before in [7], but it is limited to complete graphs with sampling dependent on all the urns and a non-linear function of the proportion of balls of white colour in each urn. Our approach naturally extends this to linear node-based sampling on more general graphs, and we aim to explore non-linear node-based sampling in future work.

2.2. Exploration process on the graph

Suppose $q_i \in \{0, 1\}$ for all $i \in [N]$ and $V = \mathcal{P} \cup \mathcal{D}$. We introduce an exploration process on the graph $\mathcal{G} = (V, \mathcal{E})$ that starts from an arbitrary node $v \in V$ and proceeds to explore its neighbours. In this process, nodes are categorised into subsets based on their sampling type and the types of nodes in their in-neighborhood. More specifically, $\mathcal{P}$ is partitioned into sets P_1 and P_2, and $\mathcal{D}$ is partitioned into D_1 and D_2, with P_1, P_2, D_1, and D_2 initially empty. Depending on v's sampling type, it is assigned to P_1 (if preferential) or D_1 (if de-preferential). In the subsequent steps, the sets P_1, P_2, D_1, D_2 are updated based on the sampling type of the newly explored node and their in-neighbours. If every node has a unique assignment, this results in a partition of V into these four disjoint subsets. The exploration process is illustrated in Figure 1. Detailed steps of the algorithm and examples are provided in the appendix (see Algorithm 1 in Appendix A). This approach thus classifies all finite directed graphs into two categories: graphs that admit partition via this exploration process and graphs that do not admit a partition.

In Section 3, we state and prove the convergence and synchronisation results for $\mathbf{Z}^t$. In particular, we show that when all $q_i \in \{0, 1\}$ the limiting behaviour of the interacting urn process depends on whether the underlying graph admits a partition or not. In Section 4, we prove CLT

https://doi.org/10.1017/jpr.2024.105 Published online by Cambridge University Press

type limit theorems for $\mathbf{Z}^t$. Finally, in Section 5, we discuss some examples with simulations and applications in opinion dynamics.

3. Convergence and synchronisation

Theorem 1. *(*Convergence of $\mathbf{Z}^t$*.) Suppose F is strongly connected and one of the following conditions holds:*

(i). *There exists a node i with $q_i \in (0, 1)$.*

(ii). *There exists a non-Pólya type node in F.*

(iii). *There are no stubborn nodes, i.e. $S \neq \varnothing$.*

(iv). *All nodes in F are Pólya type and F does not admit a valid graph partition as per Algorithm 1 (Appendix A).*

Then $\mathbf{Z}^t \xrightarrow{\text{a.s.}} \mathbf{Z}^\star$ as $t \to \infty$, where $\mathbf{Z}^\star$ is of the form $(\mathbf{Z}_F^\star, \mathbf{Z}_S^0)$ such that

$$\mathbf{Z}_F^\star = \left[\mathbf{Z}_S^0(\mathcal{I}B\widetilde{A})_{SF} + (\mathbf{a}\widetilde{A})_F - (\mathbf{q}B\widetilde{A})_F\right]\left(I - (\mathcal{I}B\widetilde{A})_F\right)^{-1}. \tag{5}$$

Remark 1. When $q_i = \frac{1}{2}$ for all i, $\mathbf{Z}_F^\star = \left(\frac{1}{2}(1 + a_1 - b_1, \ldots, 1 + a_N - b_N)\widetilde{A}\right)_F$. Further, when the reinforcement at all vertices is Pólya type ($a_i = b_i = 1$), we get $\mathbf{Z}_F^\star = \frac{1}{2}\left(\mathbf{1}\widetilde{A}\right)_F$. For instance, on a cycle graph, this special case is equivalent to N independent urns or N independent symmetric random walks.

Remark 2. We briefly discuss the case of the interacting node-based Pólya type urn process when the underlying graph does not satisfy Theorem 1(iii).

- Suppose $q_i = 0$ for all i (i.e. $\mathcal{P} = \varnothing$). Then if the graph partition exists, F admits a partition under the exploration process if and only if F is a bipartite digraph with node sets D_1 and D_2 (see Figure 1). This case is equivalent to each node i sampling uniformly and the reinforcement scheme

$$\begin{pmatrix} 0 & m_i \\ m_i & 0 \end{pmatrix}$$

  (as discussed in Section 2.1). A special case of this with $m_i = m$ for undirected bipartite graphs, specifically for urns with multiple drawings, was studied in [8].

- Suppose $q_i = 1$ for all i (i.e. $\mathcal{D} = \varnothing$). In this case, if the graph partition exists, there are two disjoint strongly connected components P_1 and P_2, with no interaction between P_1 and P_2. Since we assume that the graph is strongly connected, one of these components must be empty. A special case of this with $m_i = m$ for all i was studied in [10], where it was shown that on a regular directed graph, the limiting configuration of urns is random. Moreover, it was shown that the urns synchronise, in the sense that the fraction of balls of either colour converges to the same random limit almost surely.

In general, when the graph is regular and $m_i = m$ for all i, it is easy to see that the limiting fraction takes the form such that $Z_i^t \to Z^\infty$ for all $i \in P_1 \cup D_2$ and $Z_i^t \to 1 - Z^\infty$ for all $i \in P_2 \cup D_1$. This can be shown by swapping the colours of the balls in $P_2 \cup D_1$ and applying the existing synchronisation results from [2] for interacting Pólya urns.

https://doi.org/10.1017/jpr.2024.105 Published online by Cambridge University Press

To extend Theorem 1 for weakly connected graphs (Corollary 1), we define a strongly connected component C of F as a *stubborn block* if no node outside C can reach C; that is, for any $v \notin C$, $v \not\to C$. Otherwise, it is defined as a *flexible block*.

Corollary 1. *Suppose F is weakly connected. Suppose conditions (i), (ii), or (iv) of Theorem 1 hold for every stubborn block of F, or condition (iii) holds such that for every stubborn block F', there exists a node $s \in S$ such that $s \to F'$. Then, as $t \to \infty$, $\mathbf{Z}^t \xrightarrow{\text{a.s.}} \mathbf{Z}^\star$, where $\mathbf{Z}^\star$ is as given in (5).*

3.1. Conditions for synchronisation

We now explore the conditions for synchronisation, i.e. when the limiting fraction of balls of each colour is the same for every urn. Synchronisation occurs if and only if $\mathbf{Z}^\star_F = z^\star \mathbf{1}$ for some constant $z^\star$, therefore from (5) we get

$$z^\star\big(\mathbf{1} - (\mathcal{I}B\widetilde{A})_F\mathbf{1}\big) = \big[\mathbf{Z}^0_S(\mathcal{I}B\widetilde{A})_{SF} + (\mathbf{a}\widetilde{A})_F - (\mathbf{q}B\widetilde{A})_F\big]. \tag{6}$$

This equality holds if each element of the vectors on both sides matches, i.e., for every $i \in F$,

$$z^\star\left(1 - \frac{1}{\overline{m}_i}\sum_{j\in F\cap N_i}(2q_j - 1)r_j\right) = \frac{1}{\overline{m}_i}\left(\sum_{j\in S\cap N_i} Z^0_j(2q_j-1)r_j + \sum_{j\in N_i}\alpha_j - q_j r_j\right),$$

where $r_j = \alpha_j + \beta_j - m_j$ (which is also an eigenvalue of R_j). Therefore, the following are sufficient conditions for synchronisation.

Condition SC1. *There exists a constant μ_F such that, for all $i \in F$,*

$$\frac{1}{\overline{m}_i}\sum_{j\in F\cap N_i}(2q_j-1)r_j = \mu_F.$$

Condition SC2. *There exists a constant μ_0 such that, for all $i \in F$,*

$$\frac{1}{\overline{m}_i}\left(\sum_{j\in S\cap N_i} Z^0_j(2q_j-1)r_j + \alpha_j - q_j r_j\right) = \mu_0.$$

These conditions ensure that different components of the vector in (6) are constant, leading to synchronisation within the framework of Theorem 1. Note that $\mu_F = 1$ occurs only when $\alpha_j = \beta_j = m_j$ and $q_j = 1$ for all j, i.e. when all nodes are preferential and of Pólya type – a case not considered fully in this paper but discussed briefly in Section 5.

Another way to understand synchronisation conditions is as follows. Let

$$f_i(\mathbf{Z}^t) = \frac{1}{\overline{m}_i}\mathbb{E}\big[W_i^{t+1} - W_i^t \mid \mathcal{F}_t\big]$$

be the average proportion of white balls added to urn i at time $t+1$ given $\mathcal{F}_t$. Then, using (1) and (4), we find

https://doi.org/10.1017/jpr.2024.105 Published online by Cambridge University Press

$$\begin{aligned} f_i(\mathbf{Z}^t) &= \frac{1}{\overline{m}_i}\mathbb{E}\big[W_i^{t+1} - W_i^t \mid \mathcal{F}_t\big] \\ &= \frac{1}{\overline{m}_i}\sum_{j\in N_i}\alpha_j\big(q_j Z_j^t + (1-q_j)\big(1-Z_j^t\big)\big) + (m_j-\beta_j)\big(q_j\big(1-Z_j^t\big) + (1-q_j)Z_j\big) \\ &= \frac{1}{\overline{m}_i}\sum_{j\in N_i} Z_j^t(2q_j-1)r_j + \alpha_j - q_j r_j. \end{aligned}$$

We can decompose f_i into $f_i = f_i^{(\text{fixed})} + f_i^{(\text{random})}$, where

$$f_i^{(\text{fixed})} = \frac{1}{\overline{m}_i}\sum_{j\in N_i\cap S} Z_j^0(2q_j-1)r_j + \alpha_j - q_j r_j,$$

$$f_i^{(\text{random})} = \frac{1}{\overline{m}_i}\sum_{j\in N_i\cap F} Z_j^t(2q_j-1)r_j.$$

The synchronisation occurs when the fixed part is the same for all i and the random part changes with the same rate in the direction $(1, 1, \ldots, 1)$, which is given by

$$\big\langle \mathbf{1}, \nabla f_i^{(\text{random})}(\mathbf{Z}^t)\big\rangle = \frac{1}{\overline{m}_i}\sum_{j\in N_i\cap F}(2q_j-1)r_j.$$

Corollary 2. (Synchronisation.) *Suppose the conditions of Theorem 1 hold. Then, under the synchronisation Conditions SC1 and SC2,*

$$Z_i^t \xrightarrow{\text{a.s.}} z^\star = \frac{\mu_0}{1-\mu_F}$$

as $t\to\infty$ for every $i\in F$.

Remark 3. Note that these conditions are only sufficient and not necessary. For instance, on a cycle graph with all Pólya type nodes such that only one node is de-preferential, while condition Theorem 1(iv) holds (see also the first case discussed in Section 5.1), Condition SC1 does not hold. However, it is easy to check that the fraction of balls of either colour synchronises to a deterministic limit of $\frac{1}{2}$.

Corollary 3. (Synchronisation in extreme cases). *Suppose either condition (i), (ii), or (iii) of Theorem 1 hold. Further, suppose the following (special synchronisation) conditions hold.*

Condition SSC1. *There exist $\alpha^F, \alpha^S, \beta^F, \beta^S, m^F, m^S \in \mathbb{Z}_{\geq 0}$ with $\alpha^F + \beta^F < 2m^F + m^S$ such that, for every $i\in F$, $\sum_{j\in N_i\cap S} m_j = m^S$, $\sum_{j\in N_i\cap S}\beta_j = \beta^S$, $\sum_{j\in N_i\cap S}\alpha_j = \alpha^S$, and*

$$\sum_{j\in N_i\cap F} R_j = \begin{pmatrix} \alpha^F & m^F-\alpha^F \\ m^F-\beta^F & \beta^F \end{pmatrix}.$$

Condition SSC2. *If $S\neq\varnothing$, there exist $\alpha^{0,S}, \beta^{0,S}, m^{0,S}\in\mathbb{Z}_{\geq 0}$ such that, for every $i\in F$,*

$$\sum_{j\in N_i\cap S} Z_j^0 R_j = \begin{pmatrix} \alpha^{0,S} & m^{0,S}-\alpha^{0,S} \\ m^{0,S}-\beta^{0,S} & \beta^{0,S} \end{pmatrix}.$$

https://doi.org/10.1017/jpr.2024.105 Published online by Cambridge University Press

Then:

(i) *When there are no de-preferential nodes in the graph then, as $t \to \infty$, for all $i \in F$,*

$$Z_i^t \xrightarrow{\text{a.s.}} z^\star = \frac{m^F + m^S - \beta^F - \beta^S - \big(m^{0,S} - \alpha^{0,S} - \beta^{0,S}\big)}{2m^F + m^S - \alpha^F - \beta^F}.$$

In particular, if $S = \varnothing$ and synchronisation Condition SSC1 holds then, for every $i \in V$, as $t \to \infty$,

$$Z_i^t \xrightarrow{\text{a.s.}} \frac{m^F - \beta^F}{2m^F - \alpha^F - \beta^F}.$$

(ii) *When there are no preferential nodes in the graph,*

$$Z_i^t \xrightarrow{\text{a.s.}} z^\star = \frac{\alpha^F + \alpha^S + m^{0,S} - \alpha^{0,S} - \beta^{0,S}}{m^S + \alpha^F + \beta^F}$$

as $t \to \infty$ for every $i \in F$. In particular, if $S = \varnothing$, the fraction of white balls asymptotically synchronises to $c \in [0, 1]$ if, for all $i \in [N]$, $(1 - c) \sum_{j \in N_i} \alpha_j = c \sum_{j \in N_i} \beta_j$.

Note that in both cases, when $S = \varnothing$ the urns synchronise to $\frac{1}{2}$ provided that $\alpha^F = \beta^F$, i.e. for every $i \in [N]$, $\sum_{j \in N_i} R_j$ is a classical Friedman type replacement matrix.

3.2. Proofs

The main tool in analysing the asymptotic properties of the fraction of white balls across urns is to write an appropriate stochastic approximation scheme (see [5, 15]) for the vector $\mathbf{Z}_F^t$. Using (1) and (4), we derive the recursion for the proportion of white balls in the urn at node $i \in F$ as follows:

$$\begin{aligned} Z_i^{t+1} = \frac{1}{T_i^{t+1}} W_i^{t+1} &= \frac{T_i^t}{T_i^{t+1}} Z_i^t + \frac{1}{T_i^{t+1}} \sum_{j \in N_i} \big[\alpha_j \chi_j^{t+1} + (m_j - \beta_j)\big(1 - \chi_j^{t+1}\big)\big] \\ &= Z_i^t - \frac{\overline{m}_i}{T_i^{t+1}} Z_i^t + \frac{1}{T_i^{t+1}} \sum_{j \in N_i} m_j (a_j + b_j - 1) \chi_j^{t+1} + \frac{1}{T_i^{t+1}} \sum_{j \in N_i} m_j (1 - b_j). \end{aligned}$$

Now, we write the above recursion in vector form as follows:

$$\begin{aligned} \mathbf{Z}_F^{t+1} &= \mathbf{Z}_F^t + \big[-\mathbf{Z}_F^t + \big(\chi^{t+1} B\widetilde{A}\big)_F + ((\mathbf{1} - \mathbf{b})\widetilde{A})_F\big]\big(\overline{M}(\mathbf{T}^{t+1})^{-1}\big)_F \\ &= \mathbf{Z}_F^t + \big[-\mathbf{Z}_F^t + \big(\mathbb{E}\big[\chi^{t+1} \mid \mathcal{F}_t\big] B\widetilde{A}\big)_F + ((\mathbf{1} - \mathbf{b})\widetilde{A})_F + \big(\Delta\chi^{t+1} B\widetilde{A}\big)_F\big]\big(\overline{M}(\mathbf{T}^{t+1})^{-1}\big)_F \\ &= \mathbf{Z}_F^t + \big[h(\mathbf{Z}_F^t) + \big(\Delta\chi^{t+1} B\widetilde{A}\big)_F\big]\overline{M}_F\big(\mathbf{T}_F^{t+1}\big)^{-1} \\ &= \mathbf{Z}_F^t + \frac{1}{t+1}\big[h(\mathbf{Z}_F^t) + \big(\Delta\chi^{t+1} B\widetilde{A}\big)_F\big]\overline{M}_F + \varepsilon_t, \end{aligned} \tag{7}$$

where $\Delta\chi_j^{t+1} = \chi_j^{t+1} - \mathbb{E}\big[\chi_j^{t+1} \mid \mathcal{F}_t\big]$ is a martingale difference sequence,

$$\varepsilon_t = \mathbf{Z}_F^t + \big[h(\mathbf{Z}_F^t) + \big(\Delta\chi^{t+1} B\widetilde{A}\big)_F\big]\overline{M}_F\left(\big(\mathbf{T}_F^{t+1}\big)^{-1} - \frac{1}{t+1}\right),$$

https://doi.org/10.1017/jpr.2024.105 Published online by Cambridge University Press

and the function $h\colon [0,1]^{|F|} \to [0,1]^{|F|}$ is such that, using (2),

$$\begin{aligned} h(\mathbf{Z}_F^t) &= -\mathbf{Z}_F^t + \big(\mathbb{E}\big[\chi^{t+1} \mid \mathcal{F}_t\big]\widetilde{BA}\big)_F + \big((\mathbf{1}-\mathbf{b})\widetilde{A}\big)_F \\ &= -\mathbf{Z}_F^t + (\mathbf{Z}^t\mathbf{W})_F + \big((\mathbf{1}-\mathbf{q})\widetilde{BA}\big)_F + ((\mathbf{1}-\mathbf{b})\widetilde{A})_F \\ &= -\mathbf{Z}_F^t + (\mathbf{Z}^t\mathbf{W})_F - (\mathbf{q}\widetilde{BA})_F + ((\mathbf{1}B + (\mathbf{1}-\mathbf{b}))\widetilde{A})_F \\ &= -\mathbf{Z}_F^t + \mathbf{Z}_F^t\mathbf{W}_F + \mathbf{Z}_S^0\mathbf{W}_{SF} - (\mathbf{q}\widetilde{BA})_F + (\mathbf{a}\widetilde{A})_F. \end{aligned}$$

Thus, for $\mathbf{Z} \in [0,1]^N$,

$$h(\mathbf{Z}_F) = -\mathbf{Z}_F[I - \mathbf{W}_F] + \mathbf{Z}_S^0\mathbf{W}_{SF} + (\mathbf{a}\widetilde{A})_F - (\mathbf{q}\widetilde{BA})_F, \tag{8}$$

where $\mathbf{q} = (q_1, \ldots, q_N)$ is as defined in Theorem 1. Since $\mathbf{T}^t = \mathbf{T}^0 + t\,\overline{M}$, we have $\overline{M}_F(\mathbf{T}^t)_F^{-1} = \mathcal{O}(1/t)$. Therefore, the above recursion can be written as a stochastic approximation recursion with $\gamma_t = 1/t$ and $\{\varepsilon_t\}_{t\geq 1}$ such that $\varepsilon_t \to 0$ as $t \to \infty$. Then, from the theory of stochastic approximation [5, 15], we know that the process $\mathbf{Z}_F^t$ converges almost surely to the stable limit points of the solutions of the ordinary differential equation given by $\dot{\mathbf{z}} = h(\mathbf{z})$. Hence, from (8), whenever $I - (\mathcal{I}\widetilde{BA})_F$ is invertible, the unique equilibrium point is given by

$$\mathbf{Z}_F^\star := \big[\mathbf{Z}_S^0(\mathcal{I}\widetilde{BA})_{SF} + (\mathbf{a}\widetilde{A})_F - (\mathbf{q}\widetilde{BA})_F\big]\big(I - (\mathcal{I}\widetilde{BA})_F\big)^{-1}.$$

Hence, it is enough to show that $I - (\mathcal{I}\widetilde{BA})_F$ is invertible under the conditions of Theorem 1.

We now show that, under the conditions of Theorem 1, $I - (\mathcal{I}\widetilde{BA})_F$ is invertible.

Proof of Theorem 1. Suppose $I - (\mathcal{I}\widetilde{BA})_F$ is not invertible. Then there exists a non-zero vector $v \in \mathbb{C}^{|F|}$ satisfying $(I - (\mathcal{I}\widetilde{BA})_F)v = \mathbf{0}$. This implies that $v = (\mathcal{I}BMA\overline{M}^{-1})_F\, v$. In other words, for every $k \in F$, we have

$$\frac{v_k}{\mathcal{I}_{kk}B_{kk}} = \frac{\sum_{i\in N_k\cap F} m_i v_i}{\sum_{i\in N_k} m_i}. \tag{9}$$

Let $j = \arg\max_i |v_i|$. We denote the normalised vector v as $\tilde{v} = v/|v_j|$. Therefore, (9) can be written as

$$\frac{\tilde{v}_k}{\mathcal{I}_{kk}B_{kk}} = \frac{\sum_{i\in N_k\cap F} m_i \tilde{v}_i}{\sum_{i\in N_k} m_i} \qquad \text{for all } k \in F, \tag{10}$$

where $|\tilde{v}_k| \leq 1$ for all $k \in |F|$ and $|\tilde{v}_j| = 1$. We first show that if $|\tilde{v}_k| = 1$, then k cannot be a non-Pólya type node. From (10) we have

$$\left|\frac{\tilde{v}_k}{\mathcal{I}_{kk}B_{kk}}\right| = \left|\frac{\sum_{i\in N_k\cap F} m_i \tilde{v}_i}{\sum_{i\in N_k} m_i}\right|.$$

However, under the assumption, we have

$$\left|\frac{\tilde{v}_k}{\mathcal{I}_{kk}B_{kk}}\right| = \frac{1}{|2q_k - 1||a_k + b_k - 1|} > 1.$$

On the other hand, the right-hand side is

$$\left|\frac{\sum_{i\in N_k\cap F} m_i \tilde{v}_i}{\sum_{i\in N_k} m_i}\right| \leq 1$$

(since $\tilde{v}_i \leq 1$ for all i). This contradiction implies that k cannot be a non-Pólya type node. Now, let us consider the following cases:

https://doi.org/10.1017/jpr.2024.105 Published online by Cambridge University Press

(i) Suppose $q_j \in (0, 1)$. From (10) we have

$$\left|\frac{\tilde{v}_j}{\mathcal{I}_{jj}B_{jj}}\right| = \left|\frac{\sum_{i\in N_j\cap F} m_i\tilde{v}_i}{\sum_{i\in N_j} m_i}\right|,$$

where $\left|\sum_{i\in N_j\cap F} m_i\tilde{v}_i \,/\, \sum_{i\in N_j} m_i\right| \le 1$. However,

$$\left|\frac{\tilde{v}_j}{\mathcal{I}_{jj}B_{jj}}\right| = \left|\frac{1}{(2q_j-1)B_{jj}}\right| > 1$$

since $|B_{jj}| \le 1$ and $|2q_j - 1| < 1$. This leads to a contradiction. Now, suppose $q_r \in (0, 1)$ for some $r \ne j$. Since j is a Pólya type node, from (10) we get

$$1 = \left|\frac{\tilde{v}_j}{\mathcal{I}_{jj}B_{jj}}\right| = \left|\frac{\sum_{i\in N_j\cap F} m_i\tilde{v}_i}{\sum_{i\in N_j} m_i}\right|.$$

Considering $0 \le \sum_{i\in N_j\cap F} m_i \le \sum_{i\in N_j} m_i$ and $|\tilde{v}_i| \le 1$, the only possibility for the equality in (10) to hold is when $N_j \cap F = N_j$ and $|\tilde{v}_i| = 1$ for all $i \in N_j$. Thus, all $i \in N_j$ are also Pólya type. Now consider a directed path from r to j, denoted by $(r, i_1, i_2, \ldots, i_l, j)$. By the above argument, $r, i_1, i_2, \ldots, i_l$ are all Pólya type nodes. Now,

$$1 < \frac{1}{|2q_r - 1|} = \left|\frac{\tilde{v}_r}{\mathcal{I}_{rr}B_{rr}}\right| = \left|\frac{\sum_{i\in N_r\cap F} m_i\tilde{v}_i}{\sum_{i\in N_r} m_i}\right|,$$

which is a contradiction. For rest of the proof, we assume that $q_i \in \{0, 1\}$ for all $i \in [N]$.

(ii) We show that the theorem holds under condition Theorem 1(ii). Since j cannot be a non-Pólya type node, it follows that j must be a Pólya type node. Therefore, we have $B_{jj} = 1$ and thus from (10) we get

$$1 = \left|\frac{\tilde{v}_j}{\mathcal{I}_{jj}B_{jj}}\right| = \left|\frac{\sum_{i\in N_j\cap F} m_i\tilde{v}_i}{\sum_{i\in N_j} m_i}\right|.$$

Considering that $0 \le \sum_{i\in N_j\cap F} m_i \le \sum_{i\in N_j} m_i$ and $|\tilde{v}_i| \le 1$, the only possibility for the equality in (10) to hold is when $N_j \cap F = N_j$ and $|\tilde{v}_i| = 1$ for all $i \in N_j$. Now consider a directed path from a non-Pólya node k to j, denoted by $(i_1, \ldots, i_l)$, such that $i_1, \ldots, i_l$ are all Pólya type nodes. Such a node k and a path always exists since F is strongly connected. Then, from the previous argument, we know that $|\tilde{v}_{i_1}| = \cdots = |\tilde{v}_{i_l}| = |\tilde{v}_k| = 1$. However, this leads to a similar contradiction to earlier. Therefore, if there is at least one non-Pólya type node in F, it ensures that $I - (\mathcal{I}B\widetilde{A})_F$ is invertible.

(iii) When $S \ne \varnothing$ and there exists an $f \in F$ which is non-Pólya then, by (i), $I - (\mathcal{I}B\widetilde{A})_F$ is invertible. Now we consider the case when $S \ne \varnothing$, and all nodes in F are Pólya type. Then, by (10), we get

$$1 = \left|\frac{\tilde{v}_j}{\mathcal{I}_{jj}B_{jj}}\right| = \left|\frac{\sum_{i\in N_j\cap F} m_i\tilde{v}_i}{\sum_{i\in N_j} m_i}\right|.$$

https://doi.org/10.1017/jpr.2024.105 Published online by Cambridge University Press

This implies that $N_j \cap F = N_j$ and $|\tilde{v}_i| = 1$ for all $i \in N_j$. Note that when $S \neq \varnothing$, there exists a node $s \in S$ and $f \in F$ such that $s \to f$. Since F is strongly connected, there exists a path $f \rightsquigarrow j$, say $(f = f_0, f_1, \ldots, f_{r-1}, f_r = j)$. Along this path, for all $0 \leq m \leq r$, using the same argument as above for f_m, we get $|\tilde{v}_k| = 1$ for all $k \in N_{f_m}$ and $N_{f_m} \cap F = N_{f_m}$. However, this gives a contradiction for f_0, as $N_{f_0} \cap F \subsetneq N_{f_0}$.

(iv) Let $j = \arg\max_i |\Re(v_i)|$. We denote the normalised real part of vector v as $\bar{v} = \Re(v) \,/\, \max_i |\Re(v_i)|$. Therefore, (9) can be written as

$$\frac{\bar{v}_k}{\mathcal{I}_{kk} B_{kk}} = \frac{\sum_{i \in N_k \cap F} m_i \bar{v}_i}{\sum_{i \in N_k} m_i}, \tag{11}$$

where $|\bar{v}_k| \leq 1$ for all $k \in |F|$ and $|\bar{v}_j| = 1$. Assume that all nodes are Pólya type. In this case, we have $B = I$ and we assume $S = \varnothing$. First, suppose j is a de-preferential node. When $\bar{v}_j = 1$ then, from (11), we get

$$-1 = \frac{\bar{v}_j}{\mathcal{I}_{jj} B_{jj}} = \frac{\sum_{i \in N_j} m_i \bar{v}_i}{\sum_{i \in N_j} m_i}.$$

This implies that

$$\bar{v}_i = -1 \qquad \text{for all } i \in N_j. \tag{12}$$

Similarly, when $\bar{v}_j = -1$, from (11) we get

$$\bar{v}_i = 1 \qquad \text{for all } i \in N_j. \tag{13}$$

We now show that if $\bar{v}$ exists then there is a graph partition $\mathcal{G}(P_1, P_2, D_1, D_2)$.
From Algorithm 1 (see Appendix A), in Step 2 we initialize the sets as $D_1 = \{j\}$, $D_2 = P_1 = P_2 = \varnothing$ and repeat Steps 8 to 11 until all the nodes are covered. Then, from (12) and (13), we get $\bar{v}_i = 1$ for all $i \in D_1$, $\bar{v}_i = -1$ for all $i \in D_2$, $\bar{v}_i = 1$ for all $i \in P_1$, and $\bar{v}_i = -1$ for all $i \in P_2$. Therefore, if $\bar{v}$ exists then there can be no reassignment of nodes in Step 13, thereby resulting in a valid graph partition $\mathcal{G}(P_1, P_2, D_1, D_2)$. Similarly, when j is preferential, if $\bar{v}$ exists then a valid graph partition $\mathcal{G}(P_1, P_2, D_1, D_2)$ exists with $j \in P_1$. Therefore, $I - (\mathcal{I}B\widetilde{A})_F$ is invertible whenever F does not admit a graph partition. □

The graph exploration process in Algorithm 1 (Appendix A) is motivated by the argument given above. It is easy to see that if such a vector v exists then $P_1 = \{i \in \mathcal{P} \colon \bar{v}_i = 1\}$, $P_2 = \{i \in \mathcal{P} \colon \bar{v}_i = -1\}$, $D_1 = \{i \in \mathcal{D} \colon \bar{v}_i = 1\}$, and $D_2 = \{i \in \mathcal{D} \colon \bar{v}_i = -1\}$ forms a valid graph partition. Thus, the existence of graph partitions is equivalent to the existence of a non-zero vector v such that $(I - (\mathcal{I}B\widetilde{A})_F)v = 0$. We now prove Corollary 1, which extends the result to a weakly connected directed graph.

Proof of Corollary 1. For an arbitrary graph F with strongly connected components $F_1, \ldots, F_k$, $\widetilde{A}_F$ can be expressed as an upper block triangular matrix:

$$\widetilde{A}_F = \begin{pmatrix} \widetilde{A}_{F_1} & \widetilde{A}_{F_1 F_2} & \ldots & \widetilde{A}_{F_1 F_k} \\ 0 & \widetilde{A}_{F_2} & \ldots & \widetilde{A}_{F_2 F_k} \\ \vdots & \vdots & \ddots & \vdots \\ 0 & 0 & \ldots & \widetilde{A}_{F_k} \end{pmatrix},$$

https://doi.org/10.1017/jpr.2024.105 Published online by Cambridge University Press

where $\widetilde{A}_{F_iF_j} = M_{F_i}A_{F_iF_j}\overline{M}_{F_j}^{-1}$ is an $|F_i| \times |F_j|$ matrix such that non-diagonal blocks are not all $\mathbf{0}$. Let I_{F_i} be an $|F_i| \times |F_i|$ identity matrix. Note that $I - \mathcal{I}B\widetilde{A}$ is invertible if and only if each $I_{F_i} - (\mathcal{I}B\widetilde{A})_{F_i}$ is invertible for $1 \le i \le k$. Suppose F_r is a stubborn block; then the proof of Theorem 1 implies that $I_{F_r} - (\mathcal{I}B\widetilde{A})_{F_r}$ is invertible. Now, for a flexible block F_r, there exists a node $j \in F_r$ such that $N_j \cap F_r \subsetneq N_j$. Then, using the same argument as in case (iii) in the proof of Theorem 1, we conclude that $I_{F_r} - (\mathcal{I}B\widetilde{A})_{F_r}$ is invertible for all $1 \le r \le k$. □

Proof of Corollary 2. Synchronisation occurs when $\mathbf{Z}_F^\star = z^\star\mathbf{1}$ for some constant $z^\star \in [0, 1]$. From Theorem 1, this condition holds if

$$z^\star\mathbf{1}(I - (\mathcal{I}B\widetilde{A})_F) = \mathbf{Z}_S^0(\mathcal{I}B\widetilde{A})_{SF} + (\mathbf{e}B\widetilde{A})_F + ((\mathbf{1} - \mathbf{b})\widetilde{A})_F.$$

Then, under Conditions SC1 and SC2, we have $z^\star(1 - \mu_F)\mathbf{1} = \mu_0\mathbf{1}$. Thus,

$$z^\star = \frac{\mu_0}{1 - \mu_F}\mathbf{1}$$

is the synchronisation limit under these conditions and as $t \to \infty$. □

Proof of Corollary 3. Note that Conditions SSC1 and SSC2 imply Conditions SC1 and SC2, with

$$\mu_F = \frac{\alpha^F + \beta^F - m^F}{m^F + m^S}, \qquad \mu_0 = \frac{\alpha^{0,S} + \beta^{0,S} - m^{0,S}}{m^F + m^S} + 1 - \frac{\beta^F + \beta^S}{m^F + m^S}.$$

Therefore, synchronisation occurs and we get

$$z^\star = \frac{m^F - \beta^F - \beta^S + m^S - \left(m^{0,S} - \alpha^{0,S} - \beta^{0,S}\right)}{2m^F + m^S - \alpha^F - \beta^F}. \tag{14}$$

When $S = \varnothing$, we get

$$z^\star = \frac{m^F - \beta^F}{2m^F - \alpha^F - \beta^F}.$$

The proof for the case when all nodes are de-preferential is similar. □

Remark 4. Note that Condition SSC1 implies that if all nodes are Pólya type (i.e. $m^F = \alpha^F = \beta^F$, $m^S = \beta^S$, and $m^{0,S} = \alpha^{0,S} = \beta^{0,S}$) then there is at least one stubborn node in the in-neighbourhood of every node. In that case, (14) reduces to $\sum_{i \in N_j \cap S} Z_i^0 m_i \,/\, \sum_{i \in N_j \cap S} m_i$. Thus, the limiting fraction of white balls is a weighted average of the initial fraction of white balls in the stubborn nodes of the in-neighbourhood.

4. Fluctuation results

We now state the fluctuation results for $\mathbf{Z}_F^t$ around the almost sure limit $\mathbf{Z}_F^\star$. Suppose $\lambda_{\min}(Q)$ denotes the real part ($\Re(\cdot)$) of the eigenvalue of a matrix Q with the minimum real part. Define $\rho := \lambda_{\min}(I - \mathbf{W}_F)$, where I is a $|F| \times |F|$ identity matrix and $\mathbf{W} := \mathcal{I}B\widetilde{A}$. Note that $\mathbf{W} = \mathbf{0}$ when $\mathbf{q} = \frac{1}{2}\mathbf{1}$ (i.e. $\mathcal{I} = \mathbf{0}$). For the case when $q_i \neq \frac{1}{2}$ for all i, we assume that $\mathbf{W}$ is diagonalisable, i.e. there exists an invertible matrix U with $V = U^{-1}$ such that

$$\mathbf{W} = U\Lambda V = U\,\mathrm{Diag}\,(\lambda_1, \ldots, \lambda_{|F|}, \mathbf{0}_S)V, \tag{15}$$

https://doi.org/10.1017/jpr.2024.105 Published online by Cambridge University Press

where $\lambda_1, \ldots, \lambda_{|F|}$ are the eigenvalues of $\mathbf{W}_F$. Let column vectors $u_1, \ldots, u_N$ and row vectors $v_1, \ldots, v_N$ be the right and left eigenvectors of $\mathbf{W}$ with respect to the eigenvalues $\lambda_1, \ldots, \lambda_N$ respectively. Then $U = \begin{pmatrix} u_1 \cdots u_N \end{pmatrix}$ and $V^\top = \begin{pmatrix} v_1^\top \cdots v_N^\top \end{pmatrix}$.

Theorem 2. (Fluctuation of $\mathbf{Z}^t$.) *Suppose* $\mathbf{Z}_F^t \xrightarrow{\text{a.s.}} \mathbf{Z}_F^\star$ *as* $t \to \infty$. *Then:*

(i) *If* $\rho > \frac{1}{2}$, *as* $t \to \infty$,

$$\sqrt{t}\big(\mathbf{Z}_F^t - \mathbf{Z}_F^\star\big) \xrightarrow{\text{d}} \mathcal{N}(\mathbf{0}, \Sigma), \quad \Sigma = \int_0^\infty \big(\exp\big\{-\big(\tfrac{1}{2}I - \mathbf{W}_F\big)u\big\}\big)^\top \Gamma \exp\big\{-\big(\tfrac{1}{2}I - \mathbf{W}_F\big)u\big\}\, \mathrm{d}u. \tag{16}$$

(ii) *If* $\rho = \frac{1}{2}$ *with multiplicity 1, as* $t \to \infty$,

$$\sqrt{\frac{t}{\log(t)}}\big(\mathbf{Z}_F^t - \mathbf{Z}_F^\star\big) \xrightarrow{\text{d}} \mathcal{N}(\mathbf{0}, \Sigma), \tag{17}$$

$$\Sigma = \lim_{t\to\infty} \frac{1}{\log(t)} \int_0^{\log(t)} \big(\exp\big\{-\big(\tfrac{1}{2}I - \mathbf{W}_F\big)u\big\}\big)^\top \Gamma \exp\big\{-\big(\tfrac{1}{2}I - \mathbf{W}_F\big)u\big\}\, \mathrm{d}u.$$

Here, $\Gamma = \big(-\mathbf{W}^\top \Theta \mathbf{W} + \frac{1}{4}\widetilde{A}^\top B^2 \widetilde{A}\big)_F$ *and* Θ *is the* $N \times N$ *diagonal matrix such that* $[\Theta]_{i,i} = \big(Z_i^\star - \frac{1}{2}\big)^2$.

For $\rho < \frac{1}{2}$, we refer the reader to [15, Theorem 2.2], which states that the limit of appropriately scaled $(\mathbf{Z}_F^t - \mathbf{Z}_F^\star)$ is close to a weighted sum of some finitely many complex random vectors.

Corollary 4. *The limiting variance* Σ *can be simplified as follows:*

(i) *When* $\mathbf{q} = \frac{1}{2}\mathbf{1}$, *then (16) holds with* $\Sigma = \frac{1}{4}\big(\widetilde{A}^\top B^2 \widetilde{A}\big)_F$.

(ii) *When* $q_i \neq \frac{1}{2}$ *for all* i *and* $\mathbf{W}$ *has a decomposition as in (15) then, for* $\rho > \frac{1}{2}$, *(16) holds with* Σ *such that*

$$[\Sigma]_{ij} = \sum_{k\in F}\sum_{\ell\in F} \frac{\lambda_k \lambda_\ell}{1 - \lambda_k - \lambda_\ell}(u_k^\top \bar{\Theta} u_\ell) v_{ki} v_{lj} \quad \text{for all } i, j \in F$$

and, for $\rho = \frac{1}{2}$, *(17) holds with* $[\Sigma]_{ij} = \frac{1}{4}(u_1^\top \bar{\Theta} u_1) v_{1i} v_{1j}$. *Here,* $\bar{\Theta} = -\Theta + \frac{1}{4}\mathcal{I}^{-2}$ *is an* $N \times N$ *diagonal matrix such that* $[\bar{\Theta}]_{i,i} = -\big(Z_i^\star - \frac{1}{2}\big)^2 + \frac{1}{16}\big(q_i - \frac{1}{2}\big)^{-2}$.

Corollary 5. (Fluctuation under synchronisation.) *Suppose* $\mathbf{W} = \mathbf{W}^\top$, $q_i \neq \frac{1}{2}$ *for all* i, *and* $\mathbf{Z}^\star$ *is such that* $\bar{\Theta} = c(\mathbf{q}, \mathbf{Z}^\star)I$, *where* $c(\mathbf{q}, \mathbf{Z}^\star)$ *is a constant that depends only on* $\mathbf{q}$ *and* $\mathbf{Z}^*$. *Then:*

(i) *If* $\rho > \frac{1}{2}$, *(16) holds with* $\Sigma = c(\mathbf{q}, \mathbf{Z}^\star)\mathbf{W}^2(I - 2\mathbf{W})^{-1}$.

(ii) *If* $\rho = \frac{1}{2}$ *with multiplicity 1, (17) holds with*

$$\Sigma = c(\mathbf{q}, \mathbf{Z}^\star)\mathbf{W}^2 U^\top \begin{pmatrix} 1 & \mathbf{0} \\ \mathbf{0} & \mathbf{0} \end{pmatrix} U.$$

Further, under Condition SC1,

$$\Sigma = \frac{c(\mathbf{q}, \mathbf{Z}^\star)}{4N} J.$$

https://doi.org/10.1017/jpr.2024.105 Published online by Cambridge University Press

In particular, if synchronisation occurs, i.e. $\mathbf{Z}^\star = z^\star \mathbf{1}$ *for some* $z^\star \in [0, 1]$ *and all nodes are either preferential or de-preferential (i.e.* $q_i \in \{0, 1\}$ *for all* i*) then* $c(\mathbf{q}, \mathbf{Z}^\star) = z^\star(1 - z^\star)$.

Remark 5. (*Multiplicity of* ρ.) The fluctuation theorem (Theorem 2) gives an explicit expression for the limiting variance when $\frac{1}{2}$ is a simple eigenvalue of $\mathbf{W}$. When $\frac{1}{2}$ is not simple, a general description of the limiting variance can be found in [15]. For strongly connected F where $\mathcal{I} = I$ (all nodes are preferential), the Perron–Frobenius theorem implies that the maximal eigenvalue of $\mathbf{W}$, and therefore ρ, is simple. In the presence of de-preferential nodes, classifying graphs and reinforcement matrices that lead to $\rho = \frac{1}{2}$ as a simple eigenvalue of $\mathbf{W}$ is more complex. For instance, consider a cycle graph with n nodes with node-independent reinforcement where $\mathbf{W} = (a + b - 1)\mathcal{I}A$. In this case, certain conditions can make $\rho = \frac{1}{2}$ a simple eigenvalue. Specifically, if $q_i \in \{0, 1\}$ for all i, the characteristic polynomial of $\mathcal{I}A$ is $x^n + (-1)^{m-1}$, where m is the number of de-preferential nodes. Thus, the eigenvalues of $\mathbf{W}$ depend on the zeros of $x^n - 1$ when m is even, and zeros of $x^n + 1$ when m is odd. Since 1 is always a simple eigenvalue in the first case, $\rho = \frac{1}{2}$ can also be a simple eigenvalue. For example, in a cycle graph with eight nodes (as in Figure 10), where $\widetilde{A} = A$, the eigenvalues of $I - \mathbf{W} = I - \mathcal{I}A$ are 1, -1, $(-1 + i)/\sqrt{2}$, $(-1 - i)/\sqrt{2}$, $(1 + i)/\sqrt{2}$, $(1 - i)/\sqrt{2}$, i, $-i$. Thus, $\lambda_{\min}(I - \mathbf{W}) = \rho = \frac{1}{2}$ is a simple eigenvalue when $a + b - 1 = \frac{1}{2}$.

4.1. Proofs of fluctuation results

Proof of Theorem 2. From (8), $h(\mathbf{Z}_F) = -\mathbf{Z}_F[I - \mathbf{W}_F] + \mathbf{Z}_S^0 \mathbf{W}_{SF} + (\mathbf{a}\widetilde{A})_F - (\mathbf{q}B\widetilde{A})_F$. Thus, $\partial h(z)/\partial z = -I + \mathbf{W}_F$. Hence, when $\rho > \frac{1}{2}$, we apply [15, Theorem 2.2] and get $\sqrt{t}(\mathbf{Z}_F^t - \mathbf{Z}_F^\star) \xrightarrow{\mathrm{d}} \mathcal{N}(\mathbf{0}, \Sigma)$, where Σ is defined as

$$\Sigma = \int_0^\infty \left(\exp\left\{-\left(I - \mathbf{W}_F - \tfrac{1}{2}I\right)u\right\}\right)^\top \Gamma \exp\left\{-\left(I - \mathbf{W}_F - \tfrac{1}{2}I\right)u\right\} \mathrm{d}u.$$

Similarly, when $\rho = \frac{1}{2}$ with multiplicity 1, using [15, Theorem 2.2] we get

$$\sqrt{\frac{t}{\log(t)}}\left(\mathbf{Z}_F^t - \mathbf{Z}_F^\star\right) \xrightarrow{\mathrm{d}} \mathcal{N}(\mathbf{0}, \Sigma),$$

where Σ is defined as

$$\Sigma = \lim_{t\to\infty} \int_0^{\log(t)} \left(\exp\left\{-\left(I - \mathbf{W}_F - \tfrac{1}{2}I\right)u\right\}\right)^\top \Gamma \exp\left\{-\left(I - \mathbf{W}_F - \tfrac{1}{2}I\right)u\right\} \mathrm{d}u.$$

Here, $\Gamma = \lim_{t\to\infty} \mathbb{E}\left[\left((\Delta\chi^{t+1}B\widetilde{A})_F\right)^\top \left((\Delta\chi^{t+1}B\widetilde{A})\right)_F \mid \mathcal{F}_t\right]$. To compute Γ, we use

$$\lim_{t\to\infty} \mathbb{E}\left[\left(\Delta\chi^{t+1}B\widetilde{A}\right)^\top \left(\Delta\chi^{t+1}B\widetilde{A}\right) \mid \mathcal{F}_t\right] = (B\widetilde{A})^\top \mathbb{E}\left[\Delta\left(\chi^{t+1}\right)^\top \Delta\chi^{t+1} \mid \mathcal{F}_t\right] B\widetilde{A}.$$

From the variance expression obtained in (3) we get

$$\begin{aligned}\lim_{t\to\infty} \mathbb{E}\left[\left(\Delta\chi^{t+1}B\widetilde{A}\right)^\top \left(\Delta\chi^{t+1}B\widetilde{A}\right) \mid \mathcal{F}_t\right] &= \lim_{t\to\infty} (B\widetilde{A})^\top \operatorname{Var}\left(\Delta\chi^{t+1} \mid \mathcal{F}_t\right) B\widetilde{A} \\ &= (\mathcal{I}B\widetilde{A})^\top(-\Theta)(\mathcal{I}B\widetilde{A}) + \frac{1}{4}\widetilde{A}^\top B^2\widetilde{A} \\ &= -\mathbf{W}^\top\Theta\mathbf{W} + \frac{1}{4}\widetilde{A}^\top B^2\widetilde{A}.\end{aligned}$$

https://doi.org/10.1017/jpr.2024.105 Published online by Cambridge University Press

Thus, $\Gamma = \big(-\mathbf{W}^\top \Theta \mathbf{W} + \frac{1}{4}\widetilde{A}^\top B^2 \widetilde{A}\big)_F$. This completes the proof. □

Proof of Corollary 4. Consider the following two cases:

(i) When $\mathbf{q} = \frac{1}{2}\mathbf{1}$, we get $\mathcal{I} = \mathbf{W} = \mathbf{0}_{N\times N}$, thus $\rho = 1$ and $\Gamma = \frac{1}{4}(\widetilde{A}^\top B^2 \widetilde{A})_F$. Hence, $\sqrt{t}\big(\mathbf{Z}_F^t - \mathbf{Z}_F^\star\big) \xrightarrow{\mathrm{d}} \mathcal{N}(\mathbf{0}, \Sigma)$, where $\Sigma = \Gamma \int_0^\infty \mathrm{e}^{-u}\,\mathrm{d}u = \Gamma = \frac{1}{4}(\widetilde{A}^\top B^2 \widetilde{A})_F$.

(ii) When $q_i \neq \frac{1}{2}$ for all i, since $\mathcal{I}$ is invertible we can write $\Gamma = -\mathbf{W}^\top \Theta \mathbf{W} + \frac{1}{4}\mathbf{W}^\top \mathcal{I}^{-2}\mathbf{W} = \mathbf{W}^\top \bar{\Theta}\mathbf{W}$, where $\bar{\Theta} = -\Theta + \frac{1}{4}\mathcal{I}^{-2}$. Assuming the decomposition for $\mathbf{W}$, we have $\mathbf{W} = U\Lambda V$ with $V = U^{-1}$. Therefore,

$$\begin{aligned}\Gamma = [\mathbf{W}^\top \bar{\Theta}\mathbf{W}]_F &= (\mathbf{W}_F)^\top \bar{\Theta}_F \mathbf{W}_F + (\mathbf{W}_{SF})^\top \bar{\Theta}_S \mathbf{W}_{SF} \\ &= V_F^\top \Lambda_F \big[U_F^\top \bar{\Theta}_F U_F + U_{SF}^\top \bar{\Theta}_S U_{SF}\big]\Lambda_F V_F \\ &= V_F^\top \Lambda_F (U^\top \bar{\Theta} U)_F \Lambda_F V_F.\end{aligned}$$

Let $\tilde{\Sigma} = \big(V_F^\top\big)^{-1}\Sigma V_F^{-1}$. Then, for $\rho > \frac{1}{2}$,

$$\tilde{\Sigma} = \int_0^\infty \big(\exp\big\{-\big(\tfrac{1}{2}I - \Lambda_F\big)u\big\}\big)^\top \Lambda_F [U^\top \bar{\Theta} U]_F \Lambda_F \exp\big\{-\big(\tfrac{1}{2}I - \Lambda_F\big)u\big\}\,\mathrm{d}u.$$

For $i, j \in F$,

$$[\tilde{\Sigma}]_{ij} = \lambda_i\lambda_j\big[u_i^\top \bar{\Theta} u_j\big]\int_0^\infty \mathrm{e}^{-(1-\lambda_i-\lambda_j)u}\,\mathrm{d}u = \frac{\lambda_i\lambda_j}{1-\lambda_i-\lambda_j}\big[u_i^\top \bar{\Theta} u_j\big].$$

Hence, $\Sigma = V_F^\top \tilde{\Sigma} V_F$, where

$$[\Sigma]_{ij} = \sum_{k\in F}\sum_{\ell\in F}\frac{\lambda_k\lambda_\ell}{1-\lambda_k-\lambda_\ell}\big(u_k^\top \bar{\Theta} u_\ell\big)v_{ki}v_{lj}.$$

Now, for $\rho = \frac{1}{2}$, with $\lambda_{\max}(\mathbf{W}_F) = \lambda_1 = \frac{1}{2}$ being simple, we have

$$\tilde{\Sigma} = \lim_{t\to\infty}\frac{1}{\log(t)}\int_0^{\log(t)} \big(\exp\big\{-\big(\tfrac{1}{2}I - \Lambda_F\big)u\big\}\big)^\top \Lambda_F \big[U^\top \Theta U\big]_F \Lambda_F \big(\exp\big\{-\big(\tfrac{1}{2}I - \Lambda_F\big)u\big\}\big)\,\mathrm{d}u.$$

The (1,1) element is given by

$$\begin{aligned}[\tilde{\Sigma}]_{11} &= \lambda_1\lambda_1\big(u_1^\top \Theta u_1\big)\lim_{t\to\infty}\frac{1}{\log(t)}\int_0^{\log(t)} \mathrm{e}^{-(1-\lambda_1-\lambda_1)u}\,\mathrm{d}u \\ &= \frac{1}{4}\big(u_1^\top \Theta u_1\big)\lim_{t\to\infty}\frac{1}{\log(t)}\int_0^{\log(t)} 1\,\mathrm{d}u = \frac{1}{4}\big(u_1^\top \Theta u_1\big).\end{aligned}$$

For every other $k, l \in F$ we have $\lambda_k + \lambda_l < 1$ and thus

$$\lim_{t\to\infty}\frac{1}{\log(t)}\int_0^{\log(t)} \mathrm{e}^{-(1-\lambda_k-\lambda_l)u}\,\mathrm{d}u = 0.$$

Hence we get $[\Sigma]_{ij} = \frac{1}{4}\big(u_1^\top \Theta u_1\big)v_{1i}v_{1j}$. □

https://doi.org/10.1017/jpr.2024.105 Published online by Cambridge University Press

Proof of Corollary 5. With the assumption $\mathbf{W} = \mathbf{W}^\top$, we get $S = \varnothing$ and $U = V^\top$. Thus, for $\rho > \frac{1}{2}$, we have

$$\begin{aligned}\tilde{\Sigma} &= \int_0^\infty \left(\exp\left\{-\left(\tfrac{1}{2}I - \Lambda\right)u\right\}\right)^\top \Lambda[U^\top \bar{\Theta} U]\Lambda\left(\exp\left\{-\left(\tfrac{1}{2}I - \Lambda\right)u\right\}\right) \mathrm{d}u \\ &= c(\mathbf{q}, \mathbf{Z}^\star) \int_0^\infty \left(\exp\left\{-\left(\tfrac{1}{2}I - \Lambda\right)u\right\}\right)\Lambda^2\left(\exp\left\{-\left(\tfrac{1}{2}I - \Lambda\right)u\right\}\right) \mathrm{d}u \\ &= c(\mathbf{q}, \mathbf{Z}^\star)\Lambda^2(I - 2\Lambda)^{-1}.\end{aligned}$$

This implies that $\Sigma = c(\mathbf{q}, \mathbf{Z}^\star)V^\top \Lambda^2(I - 2\Lambda)^{-1}V = c(\mathbf{q}, \mathbf{Z}^\star)\mathbf{W}^2(I - 2\mathbf{W})^{-1}$. Now, for part (ii), i.e. when $\rho = \frac{1}{2}$, we have

$$\tilde{\Sigma} = c(\mathbf{q}, \mathbf{Z}^\star)\Lambda^2 \lim_{t\to\infty} \frac{1}{\log(t)} \int_0^{\log(t)} \mathrm{e}^{-(I-2\Lambda)u} \mathrm{d}u = c(\mathbf{q}, \mathbf{Z}^\star)\Lambda^2 \begin{pmatrix} 1 & \mathbf{0} \\ \mathbf{0} & \mathbf{0} \end{pmatrix}.$$

This implies that

$$\Sigma = c(\mathbf{q}, \mathbf{Z}^\star)\mathbf{W}^2 V^\top \begin{pmatrix} 1 & \mathbf{0} \\ \mathbf{0} & \mathbf{0} \end{pmatrix} V.$$

Thus, for $\rho > \frac{1}{2}$ we get $\Sigma = c(\mathbf{q}, \mathbf{Z}^\star)\mathbf{W}^2(I - 2\mathbf{W})^{-1}$ and for $\rho = \frac{1}{2}$ we get

$$\Sigma = c(\mathbf{q}, \mathbf{Z}^\star)\mathbf{W}^2 V^\top \begin{pmatrix} 1 & \mathbf{0} \\ \mathbf{0} & \mathbf{0} \end{pmatrix} V.$$

Further, under Condition SC1, $\sum_{i=1}^N [\mathbf{W}]_{ij} = \frac{1}{m_j} \sum_{i\in N_j} \mathcal{I}_{i,i}(\alpha_i + \beta_i - m_i) = \mu_F = \frac{1}{2}$ is the maximal eigenvalue of $\mathbf{W}$ and the corresponding normalised eigenvector is $(1/\sqrt{N})\mathbf{1}$. Hence we get

$$\Sigma = c(\mathbf{q}, \mathbf{Z}^\star)\mathbf{W}^2 V^\top \begin{pmatrix} 1 & \mathbf{0} \\ \mathbf{0} & \mathbf{0} \end{pmatrix} V = c(\mathbf{q}, \mathbf{Z}^\star)\mathbf{W}^2 \frac{1}{N} J = \frac{c(\mathbf{q}, \mathbf{Z}^\star)}{4N} J.$$

This completes the proof. □

Remark 6. When all nodes are preferential, under Condition SSC1,

$$\mathbf{Z}^\star = \frac{m^F - \beta^F}{2m^F - \alpha^F - \beta^F}$$

(note that under the conditions of Corollary 5, $S = \varnothing$). Thus, for $\rho > \frac{1}{2}$ we get

$$\Sigma = \frac{(m^F - \beta^F)(m^F - \alpha^F)}{(2m^F - \alpha^F - \beta^F)^2} \mathbf{W}^2(I - 2\mathbf{W})^{-1}$$

and for $\rho = \frac{1}{2}$ we get

$$\Sigma = \frac{\left(m^F - \beta^F\right)\left(m^F - \alpha^F\right)}{(2m^F - \alpha^F - \beta^F)^2} \mathbf{W}^2 V^\top \begin{pmatrix} 1 & \mathbf{0} \\ \mathbf{0} & \mathbf{0} \end{pmatrix} V.$$

Under Condition SSC1 with $S = \varnothing$, $\mu_F = (\alpha^F + \beta^F - m^F)/m^F$. Thus, $(\alpha^F + \beta^F - m^F)/m^F = \frac{1}{2}$ is the maximal eigenvalue of $\mathbf{W}$ with the corresponding normalised eigenvector $(1/\sqrt{N})\mathbf{1}$. Hence, we get

https://doi.org/10.1017/jpr.2024.105 Published online by Cambridge University Press

$$\Sigma = \frac{\left(m^F - \beta^F\right)\left(m^F - \alpha^F\right)}{N(m^F)^2} J.$$

Similarly, when all nodes are de-preferential we get

$$\Sigma = \frac{\alpha^F \beta^F}{N\left(\alpha^F + \beta^F\right)^2} J = \frac{4\alpha^F \beta^F}{9N(m^F)^2} J.$$

5. Simulations and discussion

Since $\mathbf{Z}_F^t$ converges to a deterministic limit under the conditions of Theorem 1, the variance $\mathrm{Var}\,(\mathbf{Z}_F^t)$ converges to zero as $t \to \infty$. Before we illustrate some examples via simulation, we obtain the approximate rate at which $\mathrm{Var}\,(\mathbf{Z}_F^t)$ converges to zero and illustrate the explicit dependence of the rate of decay on the eigenvalue structure of the matrix $\mathbf{W}_F$.

For $N \times N$ matrices Q_1 and Q_2, we write $Q_1 \preccurlyeq Q_2$ if $[Q_1]_{ij} = \mathcal{O}([Q_2]_{ij})$ for all $1 \le i, j \le N$. Further, $Q_1 \preccurlyeq f(t)$ means $[Q_1]_{ij} = \mathcal{O}(f(t))$ for all $1 \le i, j \le N$. Suppose $q_i \ne \frac{1}{2}$ for all i. From (7) and (8), recall that

$$\mathbf{Z}_F^{t+1} = \mathbf{Z}_F^t + \left[h(\mathbf{Z}_F^t) + \left(\Delta \chi^{t+1} B\widetilde{A}\right)_F\right] \overline{M}_F \left(\mathbf{T}_F^{t+1}\right)^{-1},$$

where $h(\mathbf{Z}_F) = -\mathbf{Z}_F[I - \mathbf{W}_F] + \mathbf{Z}_S^0 \mathbf{W}_{SF} + (\mathbf{a}\widetilde{A})_F - (\mathbf{q}B\widetilde{A})_F$. Therefore,

$$\mathrm{Var}\left(\mathbb{E}\left[\mathbf{Z}_F^{t+1} \mid \mathcal{F}_t\right]\right) = \mathrm{Var}\left(\mathbf{Z}_F^t + h\left(Z_F^t\right)\right) = P_t^\top \mathrm{Var}\left(\mathbf{Z}_F^t\right) P_t, \tag{18}$$

where $P_t = I - (I - \mathbf{W}_F)\overline{M}_F\left(\mathbf{T}_F^{t+1}\right)^{-1}$. Similarly, using (3) we get

$$\begin{aligned}
\mathbb{E}\left[\mathrm{Var}\left(\mathbf{Z}_F^{t+1} \mid \mathcal{F}_t\right)\right] &= \overline{M}_F\left(\mathbf{T}_F^{t+1}\right)^{-1} \left((B\widetilde{A})^\top \left(-\Theta \mathcal{I}^2 + \tfrac{1}{4} I\right) B\widetilde{A}\right)_F \overline{M}_F \left(\mathbf{T}_F^{t+1}\right)^{-1} \\
&= \overline{M}_F\left(\mathbf{T}_F^{t+1}\right)^{-1} \left(-\mathbf{W}^\top \bar{\Theta}^t \mathbf{W}\right)_F \overline{M}_F \left(\mathbf{T}_F^{t+1}\right)^{-1} \\
&= \overline{M}_F\left(\mathbf{T}_F^{t+1}\right)^{-1} (\mathbf{W}_F)^\top \bar{\Theta}_F^t \mathbf{W}_F \overline{M}_F \left(\mathbf{T}_F^{t+1}\right)^{-1} = Q_t^\top \bar{\Theta}_F^t Q_t,
\end{aligned} \tag{19}$$

where $\bar{\Theta}^t = -\Theta^t + \frac{1}{4}\mathcal{I}^{-2}$ and $Q_t = \mathbf{W}_F \overline{M}_F \left(\mathbf{T}_F^{t+1}\right)^{-1}$. Now, combining (18) and (19) we get $\mathrm{Var}\left(\mathbf{Z}_F^{t+1}\right) = P_t^\top \mathrm{Var}\left(\mathbf{Z}_F^t\right) P_t + Q_t^\top \bar{\Theta}_F^t Q_t$. Iterating this, we get

$$\mathrm{Var}\left(\mathbf{Z}_F^{t+1}\right) = \sum_{j=0}^{t} \left(\prod_{k=0}^{t-j-1} P_{t-k}^\top\right) (Q_j)^\top \bar{\Theta}_F^j Q_j \left(\prod_{k=j+1}^{t} P_k\right).$$

Since $\overline{M}_F \left(\mathbf{T}_F^{j+1}\right)^{-1} \preccurlyeq (1/j) I_F$ we get $Q_j \preccurlyeq (1/j) I_F$ and thus

$$\mathrm{Var}\left(\mathbf{Z}_F^{t+1}\right) \preccurlyeq \sum_{j=0}^{t} \frac{1}{j^2} \left(\prod_{k=0}^{t-j-1} P_{t-k}^\top\right) \bar{\Theta}_F^j \left(\prod_{k=j+1}^{t} P_k\right). \tag{20}$$

Now assuming $\mathbf{W}$ is diagonalisable, i.e. $\mathbf{W} = U \Lambda U^{-1}$, we get

$$\prod_{k=j+1}^{t} P_k \preccurlyeq U \left[\prod_{k=j+1}^{t} \left(I + \frac{1}{j}(\Lambda_F - I)\right)\right] U^{-1} \preccurlyeq \left(\frac{t}{j}\right)^{\Re(\lambda_{\max})-1}. \tag{21}$$

Thus we have the following rates of decay of variance.

https://doi.org/10.1017/jpr.2024.105 Published online by Cambridge University Press

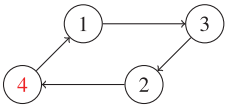


FIGURE 2. A graph with four nodes, with $\mathcal{P} = \{1, 2, 3\}$, $\mathcal{D} = \{4\}$.

Proposition 1. *Suppose $q_i \neq \frac{1}{2}$ for all i. The following bounds hold for* $\mathrm{Var}\left(\mathbf{Z}_F^t\right)$*:*

$$\mathrm{Var}\left(\mathbf{Z}_F^{t+1}\right) \preccurlyeq \begin{cases} t^{2\Re(\lambda_{\max})-2} & \text{for } \Re(\lambda_{\max}) > \frac{1}{2}, \\ t^{-1}\log t & \text{for } \Re(\lambda_{\max}) = \frac{1}{2}, \\ 1/t & \text{for } \Re(\lambda_{\max}) < \frac{1}{2}. \end{cases} \tag{22}$$

Proof. Using (21) in (20), we get

$$\mathrm{Var}\left(\mathbf{Z}_F^{t+1}\right) \preccurlyeq \sum_{j=1}^{t} \frac{1}{j^2}\left(\frac{t}{j}\right)^{2\Re(\lambda_{\max})-2},$$

which simplifies to (22) where the decay rate in the regime $\Re(\lambda_{\max}) > \frac{1}{2}$ holds because $\sum_{j=1}^{t} 1/j^{2\Re(\lambda_{\max})} < \infty$ as $t \to \infty$. □

In the next section we discuss three examples with different sampling and reinforcement schemes and present the simulation results.

5.1. Simulation results

In this section, we present the simulation results for a cycle graph with four nodes, where all the nodes are of Pólya type and $q_i \in \{0, 1\}$ for all i. We explore three specific cases for this graph.

Consider first the case when all nodes are preferential except node 4 (see Figure 2), i.e. $\mathcal{I} = \mathrm{Diag}\,(1, 1, 1, -1)$. We observe that this case satisfies condition Theorem 1(iii), as it does not have a valid graph partition. Thus by Theorem 1, $\mathbf{Z}^t$ has a deterministic limit $\frac{1}{2}\mathbf{1}$, which is independent of the initial vector $\mathbf{Z}^0$. Figure 3 illustrates the convergence of $Z_1^t, \ldots, Z_4^t$. Note that, in this case, the eigenvalues of the matrix $I - \mathbf{W}$ are

$$1 + \frac{1}{\sqrt{2}} + \frac{\mathrm{i}}{\sqrt{2}}, \quad 1 + \frac{1}{\sqrt{2}} - \frac{\mathrm{i}}{\sqrt{2}}, \quad 1 - \frac{1}{\sqrt{2}} + \frac{\mathrm{i}}{\sqrt{2}}, \quad 1 - \frac{1}{\sqrt{2}} - \frac{\mathrm{i}}{\sqrt{2}}.$$

Therefore, $\rho = 1 - (1/\sqrt{2}) < \frac{1}{2}$ and $\Re(\lambda_{\max}) = 1/\sqrt{2}$; thus, from (22) we get $\mathrm{Var}\,(\mathbf{Z}^t) \preccurlyeq t^{\sqrt{2}-2}$.

We now consider two examples of cycle graphs with four vertices where Theorem 1 does not apply. The first graph has all preferential nodes, i.e. $\mathcal{I} = \mathrm{Diag}\,(1, 1, 1, 1)$ (see Figure 4(a)). The second graph has alternate preferential and de-preferential nodes, i.e. $\mathcal{I} = \mathrm{Diag}\,(1, 1, -1, -1)$ (see Figure 4(b)). Since a valid graph partition exists according to Algorithm 1 (see Appendix A) for both cases, condition Theorem 1(iii) is not satisfied. Therefore, the urn configuration in these graphs does not converge to a deterministic limit.

The first case corresponds to a specific instance of Pólya type reinforcement at each node in a d-regular graph (where $d_i^{\mathrm{in}} = d_i^{\mathrm{out}} = d$ for all i) for $d = 2$, which was previously studied in [10]. The authors showed that synchronisation occurs, i.e. there exists a random variable Z^∞ such that $\mathbf{Z}_F^\star = Z^\infty \mathbf{1}$ (as illustrated through simulations in Figure 5).

https://doi.org/10.1017/jpr.2024.105 Published online by Cambridge University Press

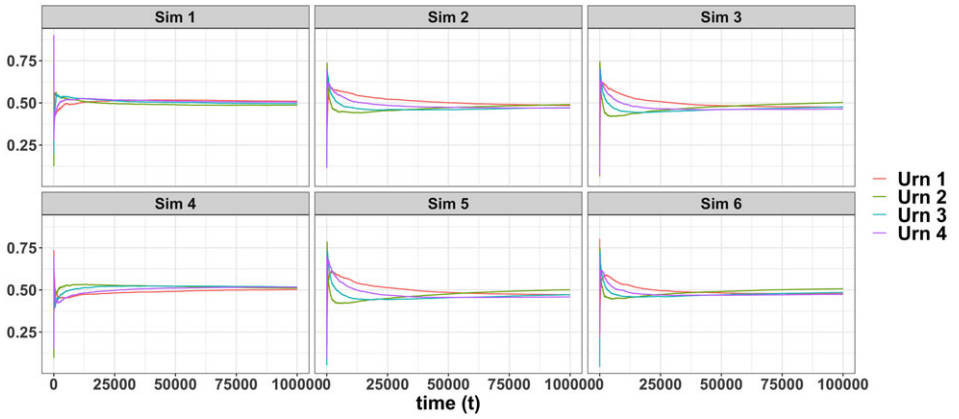


FIGURE 3. Convergence of $Z_1^t, \ldots, Z_4^t$ in six different simulations. In this case, the limit is deterministic: 0.5 for all urns.

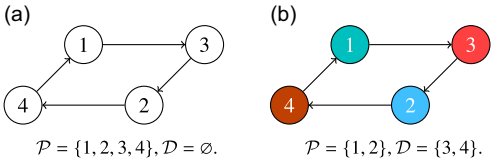


FIGURE 4. Graphs that do not satisfy the conditions of Theorem 1.

The simulations in Figure 6 suggest that in the second case, the limit is of the form $(Z^\infty, 1 - Z^\infty, 1 - Z^\infty, Z^\infty)$. This is consistent with Remark 2.

For a graph that can be partitioned using Algorithm 1 (Appendix A), the fraction of balls of either colour in each urn tends to a random limit. Specifically, from our simulations (see Figure 7), we conjecture that in a cycle graph with alternating preferential and de-preferential nodes, the limiting behaviour results in the fractions of balls of either colour in P_1, D_2 (or P_2, D_1) converging to the same limit. Further analysis of these cases, with a more general sampling scheme, is left as future work.

5.2. Application to opinion dynamics

Our model is motivated by the network-based opinion dynamics model discussed in [10]. This model uses urns to represent opinions in a network, with white and black balls indicating positive and negative views, respectively. An individual's opinion O_i^t can be represented either as a fraction Z_i^t, which is supported on [0,1], or as a sign, $\text{Sign}\left(Z_i^t - \frac{1}{2}\right) \in \{-1, 0, 1\}$. In this model, stubborn nodes are treated as bots, with Z_i^0 being the bot's power to influence towards the 'positive/favourable' opinion.

At each time step, every individual reveals their true opinion with probability q_i and reinforces their opinion based on the type of reinforcement applied: Pólya type reinforcement reinforces only the revealed opinion, whereas non-Pólya type reinforcement adds a mix of both types of views. Our main results show that on a strongly connected network if there is at

https://doi.org/10.1017/jpr.2024.105 Published online by Cambridge University Press

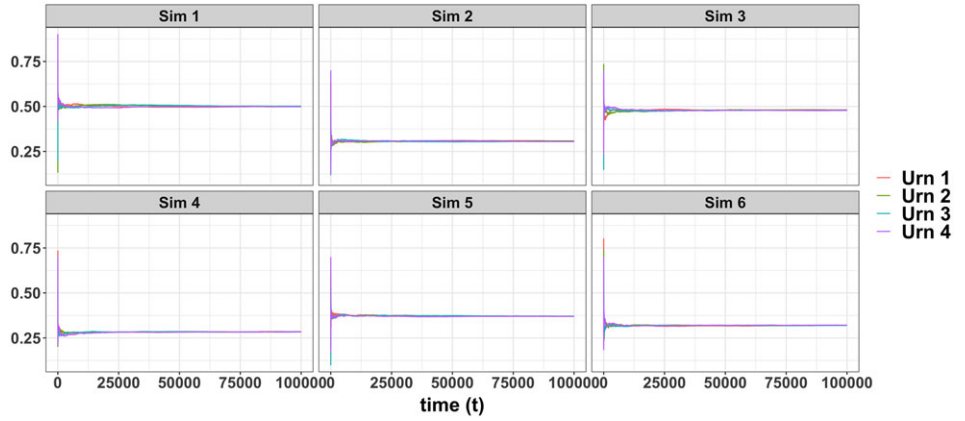


FIGURE 5. Convergence of $Z_1^t, \ldots, Z_4^t$ in six different simulations.

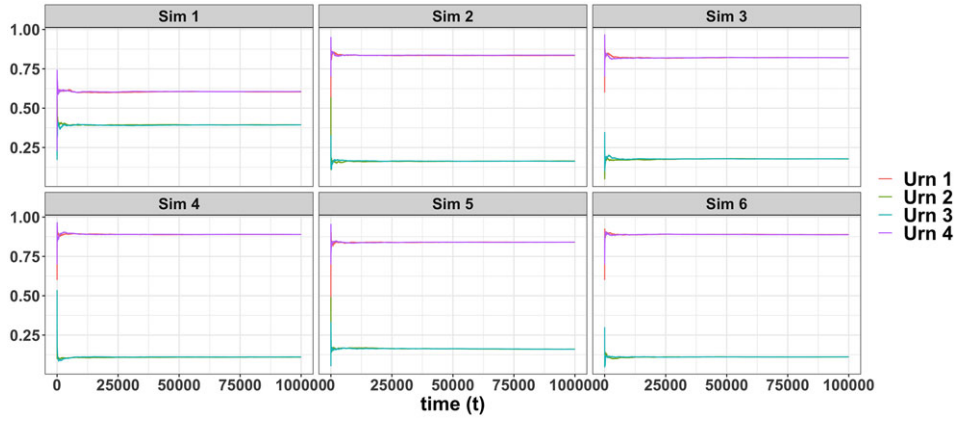


FIGURE 6. Convergence of $Z_1^t, \ldots, Z_4^t$ in six different simulations.

least one individual with $q_i \in (0, 1)$, all individuals' opinions converge to a deterministic limit. In the case when all $q_i \in \{0, 1\}$, the existence of a deterministic limiting opinion depends on the reinforcement type as well as the graph structure. We also obtain conditions for asymptotic consensus.

We briefly discuss the implications of our results for the opinion dynamics model. Consider a cycle graph on four nodes with edges $i \to i+1$ for $1 \le i \le 3$ and $4 \to 1$. Note that for directed cycles, $\widetilde{A} = A$ and therefore the m_i do not contribute to the limiting opinion. Let $x_i = (2q_i - 1)r_i'$, where $r_i' = (a_i + b_i - 1)$. The limiting opinion of node 1 is given by

$$Z_1^\star = \frac{1}{1 - x_1x_2x_3x_4}[a_4 - q_4r_4' + (a_1 - q_1r_1')x_2x_3x_4 + (a_2 - q_2r_2')x_3x_4 + (a_3 - q_3r_3')x_4].$$

Suppose, for $i \in [N]$, that $a_i = a$ and $b_i = b$. Then, $r_i' = r'$ (say) for all $1 \le i \le 4$. Further assume that $q_1 = \frac{1}{2}$. We consider two cases:

https://doi.org/10.1017/jpr.2024.105 Published online by Cambridge University Press

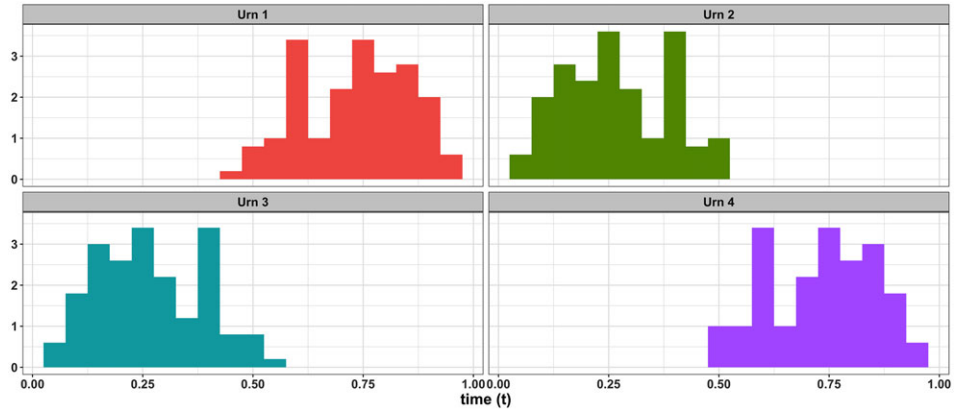


FIGURE 7. Histogram of Z_i^t in 100 different simulations, at $t = 100\,000$, for the four interacting urns placed on the nodes of the graph as in Figure 4(b).

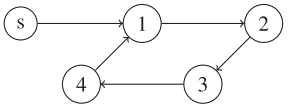


FIGURE 8. A cycle graph with a stubborn node s attached.

Case I: When all the other nodes are preferential, i.e. $2, 3, 4 \in \mathcal{P}$, we get

$$\begin{aligned} Z_1^\star(\mathrm{I}) &= 1 - b + \frac{1}{2}(1 + a - b)(r')^3 + (1 - b)(r')^2 + (1 - b)r' \\ &= \frac{a(r')^3}{2} + (1 - b)\left(1 + r' + (r')^2 + \frac{(r')^3}{2}\right). \end{aligned}$$

Case II: With $2, 3 \in \mathcal{P}$ and $4 \in \mathcal{D}$, we get

$$Z_1^\star(\mathrm{II}) = a - \frac{a(r')^3}{2} - (1 - b)\left(r' + (r')^2 + \frac{(r')^3}{2}\right).$$

Here, $Z_1^\star(\mathrm{I})$ and $Z_1^\star(\mathrm{II})$ denote the limiting configuration of urn 1 in the two cases. Note that $Z_1^\star(\mathrm{II}) = Z_1^\star(\mathrm{I})$ when $r' = 0$, and $Z_1^\star(\mathrm{II}) < Z_1^\star(\mathrm{I})$ when $r' > 0$. Now consider a bot (or a stubborn vertex s) attached to node 1, with $2, 3 \in \mathcal{P}$ and $4 \in \mathcal{D}$ (as shown in Figure 8).

In this case, the fraction of balls of white colour in urn 1 converges to $Z_1^\star(s) = Z_1(\mathrm{II}) + f\big(Z_s^0, r, \mathbf{m}\big)$, where $f\big(Z_s^0, r, \mathbf{m}\big) > 0$ for $r > 0$. Thus, a bot can be used to mitigate the effect of the de-preferential node attached to 1. Further, our results provide explicit expressions that can determine the optimal 'strength' (given by Z_s^0 and the reinforcement matrix) of the bot(s) required to obtain a specific limiting opinion profile. We remark that for a more complicated graph, the optimal positions of the bots (with varying strengths) on the network is an interesting problem in this context.

https://doi.org/10.1017/jpr.2024.105 Published online by Cambridge University Press

Algorithm 1. Graph exploration process.

Input: A directed graph $\mathcal{G}(V, E)$ and the sets of preferential nodes $\mathcal{P}$ and de-preferential nodes $\mathcal{D}$.
Output: Whether $\mathcal{G}$ admits a partition or not.

1: Select a node $j \in V$
2: **if** $j \in \mathcal{P}$ **then**
3: Initialize $P_1 \leftarrow \{j\}$, $P_2 = D_1 = D_2 = \varnothing$.
4: **else**
5: Initialize $D_1 \leftarrow \{j\}$, $P_1 = P_2 = D_2 = \varnothing$.
6: **end if**
7: **while** $(P_1 \cup P_2 \cup D_1 \cup D_2) \subsetneq V$ **do**
8: $P_1 \leftarrow P_1 \cup (\cup_{j \in P_1} N_j \cap \mathcal{P})$ and $D_1 \leftarrow D_1 \cup (\cup_{j \in P_1} N_j \cap \mathcal{D})$
9: $P_2 \leftarrow P_2 \cup (\cup_{j \in D_1} N_j \cap \mathcal{P})$ and $D_2 \leftarrow D_2 \cup (\cup_{j \in D_1} N_j \cap \mathcal{D})$
10: $P_1 \leftarrow P_1 \cup (\cup_{j \in D_2} N_j \cap \mathcal{P})$ and $D_1 \leftarrow D_1 \cup (\cup_{j \in D_2} N_j \cap \mathcal{D})$
11: $P_2 \leftarrow P_2 \cup (\cup_{j \in P_2} N_j \cap \mathcal{P})$ and $D_2 \leftarrow D_2 \cup (\cup_{j \in P_2} N_j \cap \mathcal{D})$
12: **if** P_1, P_2, D_1, D_2 are not mutually disjoint **then**
13: **BREAK** and **return** '$\mathcal{G}$ does not admit a graph partition.'
14: **end if**
15: **end while**
16: Repeat Steps 8 to Step 11 once.
17: **if** any node is reassigned from P_1 to P_2 (or vice versa) or from D_1 to D_2 (or vice versa) **then**
18: **else**
19: **return** '$\mathcal{G}$ admits a graph partition $\mathcal{G}(P_1, P_2, D_1, D_2)$ such that $\mathcal{P} = P_1 \cup P_2$ and $\mathcal{D} = D_1 \cup D_2$.'
20: **end if**

Appendix A. Graph exploration process

The graph exploration process is described in Algorithm 1. If a graph partition exists, it is determined; otherwise, the algorithm reports that no such partition is possible. Note that this partitioning algorithm is invariant to the initial choice of node j, up to a permutation of the sets (P_1, P_2, D_1, D_2). We now provide a few examples to illustrate different cases.

Example 1. (*Graph that does not admit a partition.*) Suppose $F = \mathcal{P} \cup \mathcal{D}$ is such that it is strongly connected and there is only one node in the set $\mathcal{D}$, represented as $\mathcal{D} = \{\mathfrak{d}\}$. Let $j \in \mathcal{P}$ be the node selected at Step 1 of Algorithm 1, i.e. $j \in P_1$. Since F is strongly connected, there exists a path $\mathfrak{d} \rightsquigarrow j$ such that all nodes on the path are preferential, implying that $\mathfrak{d}$ must be in set D_1 (see Step 8 of Algorithm 1). Similarly, $j \rightsquigarrow \mathfrak{d}$ via a path of preferential nodes, implying that $j \in P_2$ (see Step 9 of Algorithm 1 or see Figure 1). A similar conclusion holds if the node selected at Step 1 is $\mathfrak{d}$. Thus, such a graph does not admit a valid partition. To illustrate this, we consider a special case of a strongly connected graph with one de-preferential node in Figure 9.

Example 2. (*Graph that admits a partition.*) Consider an even cycle of size $2k$ with alternate preferential and de-preferential nodes. In this case, starting with $1 \in P_1$, the algorithm terminates with a valid assignment of nodes to the four sets, namely, $P_1 = \{1, 3, \ldots, k-1\}$,

https://doi.org/10.1017/jpr.2024.105 Published online by Cambridge University Press

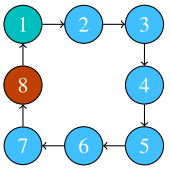


FIGURE 9. A graph with eight nodes with $\mathcal{P} = \{1, 2, 3, 4, 5, 6, 7\}$ and $\mathcal{D} = \{8\}$. Suppose in Step 3 of Algorithm 1 we initialize with $P_1 = \{1\}$, $P_2 = D_1 = D_2 = \varnothing$. Then, following algorithm Steps 8 to 11, we get $D_1 = \{8\}$ and $P_2 = \{2, 3, 4, 5, 6, 7\}$, $D_2 = \varnothing$. However, in Step 16, node 1 gets reassigned to P_2. Therefore, the graph does not admit a graph partition under Algorithm 1.

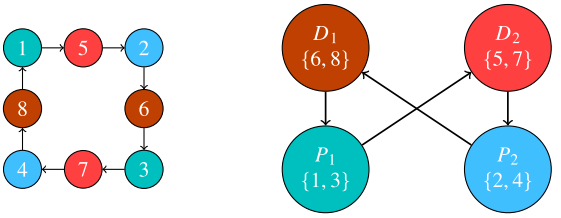


FIGURE 10. A graph with eight nodes with $\mathcal{P} = \{1, 2, 3, 4\}$ and $\mathcal{D} = \{5, 6, 7, 8\}$ that results in a valid partition via the given exploration process. In particular, we get $P_1 = \{1, 3\}$, $P_2 = \{2, 4\}$, $D_1 = \{6, 8\}$, and $D_2 = \{5, 7\}$.

$P_2 = \{2, 4, \ldots, k\}$, $D_1 = \{k+1, k+3, \ldots, 2k-1\}$, and $D_2 = \{k+2, k+4, \ldots, 2k\}$. Figure 10 illustrates the case for $k = 4$.

It is easy to see that a cycle graph with an odd number of de-preferential nodes does not admit a valid partition, whereas a cycle graph with an even number of de-preferential nodes has a valid partition.

Funding information

There are no funding bodies to thank relating to the creation of this article.

Competing interests

There were no competing interests to declare which arose during the preparation or publication process of this article.

References

[1] ALETTI, G., CRIMALDI, I. AND GHIGLIETTI, A. (2017). Synchronization of reinforced stochastic processes with a network-based interaction. *Ann. Appl. Prob.* **27**, 3787–3844.

[2] ALETTI, G., CRIMALDI, I. AND GHIGLIETTI, A. (2024). Networks of reinforced stochastic processes: A complete description of the first-order asymptotics. *Stoch. Process. Appl.* **176**, 104427.

[3] ALETTI, G. AND GHIGLIETTI, A. (2017). Interacting generalized Friedman's urn systems. *Stoch. Process. Appl.* **127**, 2650–2678.

[4] BANDYOPADHYAY, A. AND KAUR, G. (2018). Linear de-preferential urn models. *Adv. Appl. Prob.* **50**, 1176–1192.

[5] BORKAR, V. S. (2008). *Stochastic Approximation: A Dynamical Systems Viewpoint*. New York, Springer.

https://doi.org/10.1017/jpr.2024.105 Published online by Cambridge University Press

[6] CRIMALDI, I., DAI PRA, P. AND MINELLI, I. G. (2016). Fluctuation theorems for synchronization of interacting Pólya's urns. *Stoch. Process. Appl.* **126**, 930–947.
[7] CRIMALDI, I., LOUIS, P.-Y. AND MINELLI, I. G. (2023). Interacting nonlinear reinforced stochastic processes: Synchronization or non-synchronization. *Adv. Appl. Prob.* **55**, 275–320.
[8] DAHIYA, Y. AND SAHASRABUDHE, N. (2024). Urns with multiple drawings and graph-based interaction. *J. Theoret. Prob.* **37**, 3283–3316.
[9] KAUR, G. (2019). Negatively reinforced balanced urn schemes. *Adv. Appl. Math.* **105**, 48–82.
[10] KAUR, G. AND SAHASRABUDHE, N. (2023). Interacting urns on a finite directed graph. *J. Appl. Prob.* **60**, 166–188.
[11] MIREBRAHIMI, M. (2023). Synchronization and fluctuations for interacting stochastic systems with individual and collective reinforcement. *Stoch. Models* **40**, 464–501.
[12] QIN, S. (2023). Interacting urn models with strong reinforcement. Preprint, arXiv:2311.13480.
[13] SAHASRABUDHE, N. (2016). Synchronization and fluctuation theorems for interacting Friedman urns. *J. Appl. Prob.* **53**, 1221–1239.
[14] SINGH, S., ALAJAJI, F. AND GHARESIFARD, B. (2022). A finite memory interacting Pólya contagion network and its approximating dynamical systems. *SIAM J. Control Optim.* **60**, S347–S369.
[15] ZHANG, L.-X. (2016). Central limit theorems of a recursive stochastic algorithm with applications to adaptive designs. *Ann. Appl. Prob.* **26**, 3630–3658.

https://doi.org/10.1017/jpr.2024.105 Published online by Cambridge University Press